iScience

CellPress
OPEN ACCESS

Review

Igneous processes in the small bodies of the Solar System I. Asteroids and comets

Giovanni Leone[1,2,5,*] and Hiroyuki K.M. Tanaka[2,3,4]

SUMMARY

Igneous processes were quite widespread in the small bodies of the Solar System (SBSS) and were initially fueled by short-lived radioisotopes, the proto-Sun, impact heating, and differentiation heating. Once they finished, long-lived radioisotopes continued to warm the active bodies of the Earth, (possibly) Venus, and the cryovolcanism of Enceladus.

The widespread presence of olivine and pyroxenes in planets and also in SBSS suggests that they were not necessarily the product of igneous processes and they might have been recycled from previous nebular processes or entrained in comets from interstellar space. The difference in temperature between the inner and the outer Solar System has clearly favored thermal annealing of the olivine close to the proto-Sun. Transport of olivine within the Solar System probably occurred also due to protostellar jets and winds but the entrainment in SBSS from interstellar space would overcome the requirement of initial turbulent regime in the protoplanetary nebula.

INTRODUCTION

Olivine and pyroxene, minerals commonly found in lava erupted during igneous processes on Earth and in the inner planets of the Solar System, including satellites like the Moon and Io, have been found in comets and asteroids[1] of the inner and outer Solar System. Since small bodies like comets and asteroids are considered as the leftovers (or the "building blocks") of the planetary formation and they are well distributed all over the Solar System, including among the transneptunian objects (TNOs), they constitute a historical window in the evolution of the igneous processes occurred in the Solar System. We appropriately use the generic words "igneous processes" and not "volcanism" because lava from the mantle may not erupt to the surface in small bodies (i.e. asteroids or their parent bodies) with radii <190–250 km.[2] However, the typical heating processes occurring during the early formation of the planetary bodies might have been quite common all over the protoplanetary disk. Also, heating processes may have occurred in long-period comets, small bodies formed mainly in the outer Solar System where melting and igneous processes would not be that easily expected at such long distances from the Sun. The wide range of olivine (and pyroxene) compositions, minerals present in basaltic lava, directly found in comet 81P/Wild 2 grains returned by the Stardust mission suggests a wide range of formation conditions.[3–5] Olivine and pyroxene are common minerals of chondritic meteorites as well. A possibility is that the high temperatures typical of hot volcanism, necessary to melt olivine and pyroxenes, may have characterized the whole protoplanetary disk from which the Solar System was born.[6] Another possibility is simply that they were already there as condensates since the accretion of the various bodies without any particular igneous process involved. Analyzing these two options might have important implications about the distribution of primordial heating sources (PHS) all over the Solar System.[7] Three types of heating sources were available during the early formation of the Solar System: impact melting, differentiation, and radiogenic decay. Additional and favorite mechanisms of chondrule formation include shock waves and lightning. In small bodies like planetesimals and comets, melting through the first two processes is more difficult due to their small mass.[8–10] Eventual fragmentation of the planetesimals due to collisions does not hinder the formation of a significant fraction of large pebbles at the end, which leads to a lower collision rate and thus to a significantly less efficient dissipation of energy.[11,12] Impact melting is a common process for asteroid-size bodies but, at the end, radiogenic decay remains the most durable form of heating. Short-lived ^{26}Al was the most common and widespread of the PHS (i.e.[13]) at the beginning of our Solar System with ^{60}Fe[14] and ^{10}Be[15] as additional sources. Understanding the distribution of the PHS and how these affected the igneous processes of the small bodies of the Solar System is the main scope of this review.

[1]Instituto de Investigación en Astronomía y Ciencias Planetarias, Universidad de Atacama, Chile

[2]Virtual Muography Institute, Global, Tokyo, Japan

[3]International Muography Research Organization (MUOGRAPHIX), The University of Tokyo, Japan

[4]Earthquake Research Institute, The University of Tokyo, 1-1-1 Yayoi, Bunkyo, Tokyo 113-0032, Japan

[5]Present address: Instituto de Investigación en Astronomía y Ciencias Planetarias, Universidad de Atacama, Copiapó, Chile

*Correspondence: giovanni.leone@uda.cl

https://doi.org/10.1016/j.isci.2023.107160

DISTRIBUTION OF PHS IN THE SOLAR SYSTEMS PROTOPLANETARY DISK

Thanks to the many missions that have been launched so far, we have now a good knowledge of the inner and outer Solar System as far as Pluto. However, the Solar System is much more than that. Extending from the asteroid belt (AB) to the Oort cloud, as far as 2×10^{13} km or 1.33333×10^{5} au,[16] the outer Solar System is by far the largest part of the whole Solar System. A further subdivision of the outer Solar System is given by Gladman and Volk,[17] who estimate that the transneptunian space (TS) starts at 30.1 au, basically from the orbit of Neptune onward, and ends at 2,000 au where the inner Oort cloud (IOC) begins; a previous estimate found the IOC beginning at ≈ 3,000 au;[18] then, the IOC ends at 10,000 au where the outer Oort cloud (OOC) begins. There is general consensus on the OOC ending at a maximum distance of 10^5 au from the Sun, as inferred from the orbits of the long-period comets (i.e.[19–21]). This is the region where the influence of the Galactic gravitational tidal field and of the passage of neighbor stars has their own effect on the evolution of the comets.[21,22] Within the TS, it is included much of the Kuiper Belt subdivided in "classical belt", between 40 and 48 au, and the Centaurs region <30 au representing "the transition population between the short-period comets and their source region outside 30 au".[23] Unfortunately, for the TS beyond Pluto not reached by any spacecraft yet, we still have to rely on telescopic observations and spectral data, which have given great help but are still far from being comparable to the spacecraft information that we have about the inner Solar System.

The issue of the distribution of the PHS along the protoplanetary disk of our Solar System is still controversial between heterogeneous and homogeneous. Some authors favor the hypothesis of a heterogeneous distribution in the original solar nebula that may have been inherited in the protoplanetary disk with different heating effects in various parts of it.[7,24–28] The initial concentration of PHS is the key factor that determines the thermal history of the various bodies. Other authors favor a homogeneous distribution that heated uniformly the early Solar System.[29–34] Many lines of evidence point to a widespread and homogeneous distribution of ^{26}Al in the galaxy and in our Solar System.[35–37] Both hypotheses concur on the fact that chondrules' formation started early in the history of the Solar System thanks to the heating effects of the proto-Sun. However, chondrule formation may not be related to the heating events of the proto-Sun. Chondrules formed in different regions of the protoplanetary disk, inside and outside the orbit of Jupiter, and most likely by various flash-heating models: nebular lightning, magnetic reconnection flares, gas dynamic shock waves, and radiative heating.[38] If current asteroid sample return missions confirm the scarcity of chondrules observed in the preliminary results, there is a possibility that chondrules might be a rare form of preserved primordial material of the Solar System.[39] According to U-Pb chronology, chondrules' formation started almost at the same time of the condensation of the first calcium-aluminum-rich inclusions (CAIs) at 4567.3 ± 0.16 Ma,[40] which are considered the first and thus oldest solids formed in the Solar System,[41] and lasted for ≈3 Ma.[42,43] This is also the time in which the runaway accretion process formed the first rocky bodies of the Solar System from the first planetesimals,[44,45] after which giant impacts may have occurred: 1) giant impacts likely occur after the disk is dissipated;[46] 2) the runaway and oligarchic accretion (in the classic view). An example is the one that may have formed the Martian dichotomy within a time span from ≈4 to ≈15 Ma after CAI,[47] validated by the discovery of twelve volcanic alignments as postulated by the Southern Polar Giant Impact formation model,[48] or the Moon-forming impact within a time span from ≈30 to 200 Ma after CAI.[49] However, runaway accretion might not be enough to explain the dichotomy between low-mass terrestrial planets and giant gaseous planets. Accretion of drifting pebbles by embryos and cores might be the new emerging paradigm.[50–56] How this process of pebble accretion might have affected the distribution of the PHS in the evolving Solar System? Chondritic meteorites, or more generally chondrites, show limited element fractionation and differentiation after their formation in different parent bodies[57] but have been commonly considered as the building blocks for the Earth and the terrestrial planets.[58–62] However, it is unlikely that chondrites alone formed the Earth; the addition of other chemically distinct small bodies from the bulk Solar System composition has been proposed.[57,63–65] Recent geochemical analyses in meteorites have shown that the inner and the outer Solar System may have formed from two distinct reservoirs of planetesimals,[66–68] which may reflect the difference in the initial abundance of ^{26}Al found in chondrites.[69] The isotopic dichotomy between non-carbonaceous chondrites (NC) and carbonaceous chondrites (CC) indicates how the two distinct reservoirs from which they formed remained separated during the first few millions of years; the NC inside the orbit of Jupiter, the CC outside the orbit of Jupiter.[70] The isotopic dichotomy between CC and NC meteorites is observed not only for chondrites but also for achondrites. Achondrites provide key arguments for an early separation of the isotopically distinct reservoirs, possibly by proto-Jupiter.[71] Different abundances of neutron-rich isotopes such as ^{54}Cr, ^{50}Ti, and ^{48}Ca in different bodies of the inner Solar System suggest a heterogeneous distribution

of pre-solar grains attributed to an early solar irradiation.[72] Migration of the giant planets may also have contributed to capture TS planetesimals, as it was suggested for Phoebe,[73] and increase collisions among planetesimals thus mixing up the original distribution.[74]

Observations of other protoplanetary disks around other forming planetary systems show that the population of planetesimals in our Solar System represents one of the many possible combinations defined by the wide range of C/O ratio and metallicities present in other interstellar nebulas, which significantly affects the formation of water ice and refractory phases in icy planetesimals; "planetesimals in systems with sub-solar C/O should be water ice-rich, with lower than solar mass fractions of refractory materials, while in super-solar C/O systems planetesimals should have significantly higher mass fractions of refractories, in some cases having little or no water ice.".[75] The evidence that extrasolar asteroids show a variation in iron to aluminum ratio over a factor of 100 unequivocally shows that they have undergone igneous differentiation due to heating produced by ^{26}Al and thus it should be regarded as a quite common PHS in other stellar systems as well.[13]

IGNEOUS PROCESSES IN ASTEROIDS

Igneous processes in asteroids were already reviewed by McSween,[1] who noticed how fractional crystallization is a "pervasive process that probably affects primary magmas generated within bodies of virtually any size." He noticed that fractionation and subsequent differentiation processes at the low (lithostatic) pressures typical of asteroids still produced eucrites, basaltic rocks which constitute the largest group of achondritic meteorites, and ureilites, ultramafic rocks containing olivine and pigeonite whose isotopic compositions resemble those found in CC.[1] However, ureilites fall in the NC range in terms of isotope compositions. Actually, they are more "non-carbonaceous" (i.e., further from the CC end in the stable isotope composition plots) than any other material.[67] Some CC, those belonging to the CV group, are also rich in CAIs.[57,76] Wilson and Keil[2] put some limit to the size of the small bodies, with radii <190–250 km, in which lava from the mantle may not erupt to the surface. Greenwood et al.[77] have raised geochemical arguments about the possible existence of magma oceans on differentiated asteroids whereas Mayne et al.[78,79] argued that 4 Vesta, for example, is too inhomogeneous to be the result of differentiation of a global magma ocean. Wilson et al.[80] found how difficult is generating >30% of total melting in the ureilite parent body because of efficient melt removal from its interior. However, the idea that melt migration was efficient enough to remove ^{26}Al, and thus dampen the melting, relied on overestimated percolation rates so that such a drainage cannot prevent the possible formation of global magma oceans.[81] There are even some more recent results of experiments in low-degree (<15%) partial melts rich in SiO_2, Al_2O_3, and alkali elements that suggest the possibility of widespread high-viscosity silica-rich melts in small bodies of the early Solar System but that the evidence was erased by subsequent stages of melting, accretion, and differentiation.[82] "Primitive achondrites may record melt migration in rubble-pile bodies reaccreted from fragments of partially molten planetesimals."[83] Thus, it is very likely that some asteroids were more chemically modified respect to others with chondrites generally less differentiated than achondrites.[57]

There is a class of CAI-rich asteroids of the Watsonia family, which have affinity with the fluffy type As CAI, that have not experienced melting before accretion during the first half-life of ^{26}Al.[84] To explain such exception, it was suggested that ^{26}Al was not yet present in our Solar System at the time of formation of these asteroids and that probably was injected afterward by a stellar source[85] although modeling results showed how such injection from the stellar shock front would take $\approx 2–4 \times 10^5$ years before that short-lived nuclides can enter the collapsing protosolar cloud via Rayleigh-Taylor instability.[86,87] A possible explanation could thus be that only the region of formation of the Watsonia family asteroids was possibly devoid of ^{26}Al.[84,87] Compositional variations, particular in olivine, with heliocentric distance have been observed even within the AB thus reflecting compositional differences and different melting histories already since the time of formation from the primordial nebula.[88] We will thus explore the situation in the various asteroids of the Solar System to understand whether these are isolated or common cases. We mainly refer to the Tholen taxonomy[89] in our description.

Igneous processes in C-type asteroids

Information about C-type asteroids mainly comes from meteorites found on Earth but now also from sample return missions like Hayabusa2 to Ryugu and the Origins, Spectral Interpretation, Resource Identification, and Security-Regolith Explorer (OSIRIS-REx) to Bennu missions. C-type asteroids, which include

B-type, F-type, and G-type, are mostly found at the outer edge of the AB and are considered as among the most primitive extraterrestrial materials that experienced extensive aqueous alteration.[90] They have spectra rich in hydrated minerals very similar to those of CI and CM chondrites as well as 70% of CR chondrites,[90–92] but they also occur as near-Earth asteroids as in the case of Ryugu (i.e[93]) and Bennu (i.e.[94]). CI and CM chondrites contain Fe and Mg-phyllosilicates, mostly resulting from the aqueous alteration of olivine,[95,96] but also grains of pyroxenes and olivine preserved from aqueous alteration as contained in CAIs and ameboid olivine aggregates (AOAs).[90,97–99] The origin of these AOAs has already been matter of study, one possibility is crystallization from a chondrule melt,[100–102] another possibility is direct condensation from a solar nebular gas,[103,104] another one is a repeated sequence of mixing and partial melting[105] and, at last, splashing out from still partially molten chondrules,[106,107] or simply aggregational objects composed of CAIs and forsterite plus Fe,Ni-metal condensates (AOAs have solar-like O-isotope compositions, whereas chondrules are depleted in ^{16}O).[104] Three out of five of these processes require a heat source and, whatever it is the most plausible among these processes, a possible primordial heat source may likely be ^{26}Al along with ^{60}Fe or short duration heating followed by slow cooling (thermal annealing) near the proto-Sun. Impact plume origin of chondrules is one of the possible mechanisms of chondrule formation, it is generally accepted for CB and some CH chondrules.[108] It was also suggested that CC are significantly younger than ordinary chondrites (OC) and enstatite chondrites, which were heated by short-lived radiogenic elements; after ^{26}Al and ^{60}Fe had become extinct, the primitive dust accreting at low temperatures would have been mixed to varying quantities of high-temperature chondritic minerals ("owing to explosive volcanism and collisions"), thus forming the mineral assemblages actually found in most CC.[109]

A review of the possible origin of CC has shown how they may likely come from asteroids rather than from comets because they have undergone various processes typical of the inner rather than the outer Solar System during their history: implanted solar wind gases, microcraters, solar flare tracks, and anisotropically irradiated grains.[110,111] Furthermore, petrographic analyses have shown how thermal metamorphism affected CO and CV chondrites while CI, CM, and CR chondrites have undergone low-temperature aqueous alteration.[92,94–99,111] This means that C-type asteroids, which these meteorites come from, have undergone both the same processes implying ongoing igneous processes during their early stages of formation. Which one is the most likely heating source, radiogenic vs. impact, may come from the information acquired by the sample return missions (i.e.[112]).

101955 Bennu

101955 Bennu was taxonomically classified as a member of the rare B-type asteroid class[113–115] and appears in the images as a rubble pile of 492 $\pm$ 20 m of diameter,[116,117] considered as the best analog for CM1 chondrule poor meteorites.[118] However, the measured density of 1,190 $\pm$ 13 kg m^{-3} [116,119] is much lower than CI meteorites.[39] The high bulk porosity (from 40% to 50%) suggests that its interior is a mixture of boulders and voids,[119] and the lack of significant topographic relief indicates that 101955 Bennu might be a rubble-pile asteroid.[117] Given the short collisional lifetime (~0.1–1 Ga[117]) of a sub-kilometer-sized object in the main AB, it is thought to have originated from a larger carbonaceous asteroid of ~100 km, either of the 495 Eulalia[120] or the 142 Polana family[121,122] located in the AB at a distance of 2.42 au from the Sun,[115,120] after a catastrophic fragmentation probably occurred around 0.7–2.0 Ga ago.[123] Subsequently to its formation, 101955 Bennu was likely placed in its current position as NEA by inward drifting caused by the so-called Yarkovsky-O'Keefe-Radzievskii-Paddack (YORP) thermal effect.[120,123]

Compositionally, 101955 Bennu is a CC and its B-type classification allows comparisons of its spectral properties with other members of its class. As possible analogs, 24 Themis[124,125] and comet 133P/Elst-Pizarro,[126] as well as CI and CM chondrites,[118] were taken in consideration due to their content of water ice and organics, thus suggesting that 101955 Bennu may contain similar materials.[120] Unfortunately, the arrival of the sample return mission to Earth is expected for September 2023;[120] we need to wait for the analyses of the sample in order to have more detailed information on Bennu's composition. Partial least squares modeling of spectral data coming from the OSIRIS-REx mission has confirmed the presence of 78% of phyllosilicates and 9% of olivine, consistent with CI/CM chondrites mineralogy that have undergone aqueous alteration and thermal metamorphism.[127] However, thermal metamorphism indicates that the meteorites were once baked, but not necessarily melted. Chondrites are classified into different petrologic types, according to their levels of thermal metamorphism:[128] Type 1–2 chondrites mainly underwent aqueous alteration; type 3 chondrites experienced low-degree thermal metamorphism (less than

~600°C); types 4–6 chondrites reached higher temperatures, but with an upper limit defined by the onset of melting (~950°C). Although most chondrites have more or less undergone thermal metamorphism, they have not experienced silicate melting. Indeed, silicate melting has been suggested as the transition between chondrites and achondrites.[130] The concept of chondrites as metamorphic rocks was already studied by Wood[129] in the early 60s coming to the conclusion that the process of thermal metamorphism should have occurred in a (larger) parent body which was heated by short-lived radiogenic elements like ^{26}Al. The chondrule must have cooled as liquid droplet and then dispersed in space or in a gas where it took its spherical shape.[129] The sequence of events that have shaped 101955 Bennu has been synthesized by Lauretta et al.[120]: a) formation of pre-solar grains with water ice and possible organics in a nebula; b) mineral assemblage in the Solar System's protoplanetary disk; c) accretion of the ~100 km parent body within 10 Ma after CAI, large enough to retain the heat produced by the short-lived radiogenic elements and allow aqueous alteration and thermal metamorphism; d) disruption of the parent body by a catastrophic collision and subsequent formation of 101955 Bennu as a rubble-pile asteroid; e) drifting to Earth by YORP effect and stabilizing current position by secular resonance; f) reshaping of orbit and surface by close planetary encounters.

162173 Ryugu

162173 Ryugu is also a C-type asteroid with a global average density of 1,190 ± 20 kg m^{-3},[131–133] which is strikingly similar to that of 101955 Bennu. They share the Tholen sub-classification as B-type[134] although 162173 Ryugu shows an average bulk density of 1,282 ± 231 kg m^{-3} in the sample particles returned last December 6, 2020.[135] As well as in the case of 101955 Bennu, such a density is quite lower than the anomalous and compositionally similar CI no-chondrite meteorites (1,660 ± 80 kg m^{-3})[136] found at Tagish Lake, the most porous found on Earth, thus implying that 162173 Ryugu must also be highly porous up to 46%,[135] 50%,[131] or even 55%.[137] Other samples resulted denser than 1,800 kg m^{-3},[135] which is slightly more than the one encountered in the Tagish Lake meteorite, but still far away from the typical density (i.e. > 3,000 kg m^{-3}) of other meteorites found on Earth.[138] The most recent analyses of Ryugu samples provided an average density of 1,528 ± 242 kg m^{-3}, which does not differ much from that of the Orgueil or Tagish Lake meteorites.[139] The absence of chondrules in the samples[135] may suggest that they might be uncommon in 162173 Ryugu material and in primordial materials as well, where the abundance of chondrules might have been overestimated.[39] Such a conclusion was drawn also on the basis of the observation that the flux of meteorites making to the surface of Earth through the atmospheric barrier is just ~0.15 metric tons per day, which is less than 0.1%–0.5% of the 30–180 metric tons of material reaching the Earth.[39,140] The decreasing reflectance spectra between 0.5 and 0.8 μm in the chondrules found in the Murchison meteorite are certainly due to olivine[141] and a similar reflectance drop was attributed to olivine in 162173 Ryugu.[142] However, it is not yet certain that olivine will be present on 162173 Ryugu in amounts that might reveal the possible presence of aggregates like chondrules. The slight density variation found in samples of the same asteroid may indicate a mixture of particles of different origin,[143] or different degree of alteration,[135] or evidence of differentiation in the parent body identified as either 495 Eulalia or 142 Polana family[144] as in the case of 101955 Bennu. Basically, it is a parallel or similar history of the asteroid 101955 Bennu[134] even though the abundance of phyllosilicates and olivine might not be the same. The low degree of hydration found in partially hydrated minerals of the available samples suggests that the parent body from which 162173 Ryugu formed was water poor.[131] However, a more recent paper by Nakamura et al.,[145] based on the returned sample taken from the surface of Ryugu, shows that this asteroid experienced extensive aqueous alteration. An alternative explanation could be that 162173 Ryugu was never part of a larger parent body but simply formed from an assemblage of chondrule-free primordial blocks that was never lithified, in such a case it would not be a rubble-pile asteroid[39] like 101955 Bennu. Alternatively, the low abundance of chondrules in Ryugu samples can be simply explained by a scarcity of chondrules in its original location of formation.[146] Other suggested scenarios involve both incipient and aqueous alteration of the parent body with subsequent dehydration by internal (^{26}Al) or impact heating then followed by the classic disruption of the parent body and re-assemblage as rubble-pile asteroid.[131]

Igneous processes in the asteroid 4 Vesta (V-type)

4 Vesta, with its 262.7 ± 0.1 km in radius, is considered more a surviving intact protoplanet rather than an asteroid; it has an average bulk density of 3,456 ± 1% kg m^{-3} and a constrained core size between 107 and 130 km in radius.[147,148] Its radius places 4 Vesta slightly above the limit of the bodies that can theoretically have direct eruptions from the mantle to the surface, as suggested by Wilson and Keil.[2] Although 4 Vesta has been regarded as the parent body for the V-type asteroids, thought to be genetically related to the

howardite-eucrite-diogenite (HED) asteroids as collisional fragments coming from the surface of 4 Vesta,[149] a statistical analysis showed how such a surface compositional compatibility with the parent body is met in the inner AB but not in both middle and outer AB V-types.[150] The unexpected discovery of olivine in Albana, Arruntia, Bellicia, Caparronia, Manilia, and Pomponia craters of 4 Vesta suggests the presence of crustal plutons whose outcrops could be detected on the surface.[151,152] Eu anomalies displayed by the diogenites strongly indicate that they intruded the eucritic crust thus being younger rather than older as previously expected.[153] Pre-Dawn observations based on HED meteorites suggested a minor content of olivine in diogenites, except a few ones with higher abundances of harzburgites,[153] and mostly confined in the mantle,[154] or at the base of the crust,[153] and thus being older than eucrites as suggested by available differentiation models.[151] However, the deepest regions in the Rheasilvia basin reaching the mantle of Vesta, where olivine should have been largely expected, did not show clear detections.[152] Alternative models suggested that diogenites formed during the cooling of the magma ocean and then intruded the eucritic crust in the northern regions of Vesta.[153,155,156] From the available maps, such intrusions are also visible in the southern regions but the formation of Veneneia and Rheasilvia basins probably deleted the traces although the impacts should have caused some reshuffling of previous terrains.[152]

A thermal model for the differentiation of the asteroid 4 Vesta was based on an initial concentration of 1.69–6.68 wt % of ^{26}Al in the eucritic crust and barren mantle as end members, respectively, and 14.62–89.34 wt % ^{60}Fe segregated in the eucritic crust and core as end members, respectively; the time of core formation moves forward or backward by 0.72 Ma (the half-life of ^{26}Al) upon increase of 100% or decrease of 50% with respect to the initial conditions of ^{26}Al abundance.[157] According to the results of this model, accretion ended at 2.85 $\pm$ 0.05 Ma after CAI, core formation occurred at 4.58 $\pm$ 0.05 Ma, and crust formation at 6.58 $\pm$ 0.05 Ma in order to achieve 25% of partial melting by decay of ^{26}Al. The heating effect of ^{60}Fe was found to be negligible. The parameters of the model were based on the assumption that the geochemistry and chronology of 4 Vesta are constrained by HED,[157] which are achondritic meteorites.[1] The initial ^{26}Al/^{27}Al ratio was assumed according to the canonical value of 5×10^{-5}.[87,157] Another thermal model for the differentiation of 4 Vesta[158] adopted an initial concentration of 1.19 wt % of ^{26}Al and 11.18 wt % of ^{60}Fe, same initial ^{26}Al/^{27}Al ratio of 5×10^{-5} and a ^{60}Fe/^{56}Fe ratio of 1.6×10^{-6}. The results of this model show a range for accretion time between 1 and 2.6 Ma after CAI, differentiation time ranges between 0.17 and 1.72 Ma after accretion, and core formation is completed 0.3 Ma after the last stage of silicate-metal differentiation.

HED are anhydrous meteorites considered as the best example of materials derived from 4 Vesta[1,159] but existing deviations from oxygen isotopic composition from a common mass-fractionation line suggest that some of them may derive from other bodies.[160] The geochemistry of HED meteorites indicated that 4 Vesta is depleted in volatiles but has some abundances in chondritic refractory elements, despite HED being essentially achondritic, and supports the model of a possible magma ocean; the geochronology indicates accretion and differentiation of 4 Vesta in the first several Ma, consistent with other small bodies of the Solar System (i.e.[161,162]) and even Mars due to its peculiar giant impact that accelerated the core formation and thus its differentiation process (i.e.[47]). Based on ^{53}Mn-^{53} Cr systematics, Lugmair and Shukolyukov[163] concluded that the HED parent body (that is, 4 Vesta) was completely molten and differentiated within 1 Ma after CAI[164] while igneous processes lasted for just $\approx$10 Ma with a total thermal history of probably $\approx$100 Ma.[160] A recent petrologic study of apatite within unbrecciated and monomict eucrites suggested how the volatile depletion that characterized 4 Vesta was not solely due to the degassing of eucritic melts in a global magma ocean but was already present in the precursor materials that accreted to form it.[165]

Igneous processes in S-type asteroids

Stony (S-type) asteroids are made of unmelted nebular materials typical of chondrites with petrologic histories significantly different from those characterizing totally melted achondrites like the HED asteroids and significant progress has been made in order to identify possible parent bodies.[166] However, exceptions were found thus making more complex the reconstruction of the genealogic trees of several asteroids. High-calcium pyroxene with minor amounts (<20%) of olivine was detected in spectra of S-type asteroids 17 Thetis, 808 Merxia, 847 Agnia, and the main belt asteroid 1489 Magnya, thus providing a strong evidence for melting and igneous differentiation in a precursor of chondritic composition.[167] Magnya, in particular, was found in the outer main belt in a region too far away from 4 Vesta to be somehow dynamically connected with it.[168] Only the S(IV)-subtype asteroids (mostly located in the Kirkwood Gap at 2.5 au) show

silicates of some consistency with ordinary chondrites (OC), all the other subtypes from S(I) to S(VII) show assemblages of silicates ranging from dunites (olivine) to pure pyroxene and mixtures of pyroxene and feldspars.[169] For the S(IV), several possible parent bodies have been identified: 3 Juno (89% H-type OC), 7 Iris (97.5% LL-type OC), 25 Phocaea (98.6% H-type OC),[170] and 6 Hebe.[171]

6 Hebe has also been found as the possible parent body of the H-type OC and of the IIE iron meteorites.[172] A thermal model for 6 Hebe, based on the same assumptions made for 4 Vesta (that is, the classic ^{26}Al decay with a "canonical" chondritic abundance given by the starting ratio of $^{26}Al/^{27}Al = 5 \times 10^{-5}$), found a range of accretion times from 6 to 8 Ma reaching the peak temperature of 1223 K.[171] Another study, although acknowledging that 6 Hebe may be the parent body of the H-chondrites, points out that its high bulk density is difficult to reconcile with pure H-chondrite material and suggests a body with a radius no larger than 130 km; body that, by the way, is consistent with the radius of 3 Juno and whose accretion took no more than 0.2 My after CAI with a peak temperature of 1180 K.[173] Best fit models for the H chondrite parent asteroid indicate that ^{26}Al was the main heat source fueling thermal metamorphism, with a marginal contribution of ^{60}Fe, without reaching partial differentiation, with formation age of 2 Ma after CAI.[174] In the case of 6 Hebe, the heat retention was prolonged to 60 Ma.[175]

The observation of 243 Ida, 433 Eros, and 951 Gaspra has shown fractured but coherent bodies that are in conflict with existing models of formation as bound aggregates of rubble; "these conflicting views may be reconciled if 10–50 km S-type asteroids formed as rubble piles, but were later consolidated into coherent bodies" through lithification by metamorphism or injected impact melt.[176] Effectively, the heat retention in brecciated bodies like aggregates of rubble could be long, unless they are excavated by collisions provoking rapid cooling; however, in the case of 951 Gaspra, the cooling was quite rapid also due to its small dimensions (~20 km diameter) with a heat retention no more than four half-lives of ^{26}Al.[175]

25143 Itokawa

The rubble-pile asteroid 25143 Itokawa is an ellipsoid with diameters of 535 (X) by 294 (Y) by 209 (Z) m, with an average bulk density of 1,940 $\pm$ 140 kg m^{-3},[177] and was explored by the Hayabusa mission in November 2005 with two touchdowns for sample return purposes.[178] Including the smooth surface at the Muses Sea, this asteroid shows large boulders on its surface with evidence of movement of material suggesting dynamic events on shorter timescales (i.e. ~ 10 Ma) than its residence near the Earth.[179–181] The movements are consistent with impact-induced vibrations produced by even centimeter-sized impactors.[180] The preliminary X-ray fluorescence data coming from the Hayabusa mission essentially confirmed previous ground-based data in which 25143 Itokawa was spectroscopically classified as S(IV) asteroid showing affinities with LL-chondrites, although some primitive achondrites cannot be ruled out.[182] The analyzed samples returned on Earth in June 2010, which were three grains of mainly crystalline olivine with dimensions between 40 and 60 μm, showed that the asteroid experienced solar wind irradiations for "a time long enough to accumulate large amounts of solar particles".[183] The olivine experienced thermal annealing, it was heated up to a temperature of 1073 K, and then cooled slowly at a rate of ~0.5 K for 1000 years to reach a temperature of 873 K; this slow cooling probably occurred in a parent asteroid larger than 25 km.[184] The small size of 25143 Itokawa and the petrology of its silicates suggest that such a larger S-type parent body may have experienced significant thermal metamorphism, disaggregation by impact, and then re-accretion of the small pieces into the reduced size rubble pile observed today.[179] Petrologic data from samples of Muses Sea confirm that 25143 Itokawa is an OC LL4 to LL6.[184]

Igneous processes in M-type asteroids

The M-type asteroids are characterized by a moderate albedo ($0.10 < p_v < 0.30$) and are a subgroup of the X-type asteroids, which also include the high-albedo ($p_v > 0.30$) E-type and the low-albedo ($p_v < 0.10$) P-type asteroids.[185–187] Although asteroids referring to the M-type are thought to be entirely metallic, some spectroscopic absorption features confirm that several asteroids do not have a pure metallic composition.[188] In fact, the average density of the denser X_c-types is around 4.9 kg m^{-3} and the density of the X-types is around 1.8 kg m^{-3}.[189] The densities of M-type asteroids are usually less than half the density of iron.[189–191] This evidence would challenge the view that M-type asteroids are largely metallic, they are probably metallic rubble piles.[192] Another good method to observe M-type asteroids is through radar, which is useful to identify metal content.[187] A survey of 14 M-type asteroids done through the Arecibo Observatory's S-band (12.6 cm) radar found that only 16 Psyche, 216 Kleopatra, 347 Pariana, 758 Mancunia, 779 Nina, and 785 Zwetana have a dominant metallic composition while 129 Antigone may

be a CH/CB/Bencubbinite body; 22 Kalliope, 97 Klotho, 110 Lydia, 224 Oceana, 678 Fredegundis, 771 Libera, and 796 Sarita showed higher radar albedo than the average AB and thus a significant metal content was not ruled out; 21 Lutetia, 135 Hertha, and 497 Iva showed the lowest metal abundances.[188,193,194] Other previous studies have found that M-type asteroids may have been formed as a mixture of different compositions such as iron with low-Fe silicates, enstatite chondrites, and carbonaceous chondrites.[195–197] Near-infrared absorption features in the ≈0.9 μm spectral region were reported for 16 Psyche, 69 Hesperia, 110 Lydia, 125 Liberatrix, 201 Penelope, and 216 Kleopatra; these features were interpreted as evidence for the presence of orthopyroxenes and relatively reducing conditions in their parent bodies or nebular regions during their formation.[198] A subsequent study revealed that 27 out of 45 M-type asteroids show absorption features attributable to pyroxenes, olivine, phyllosilicates, and hydroxides.[199] Among these asteroids, which were originally interpreted as being dry,[200] 216 Kleopatra and 418 Alemannia showed the presence of hydrated minerals.[185] Further interpretations for the origin of these asteroids include: 1) possible fragments of metallic cores of their differentiated parent bodies being the orthopyroxene, a residual of the mantle; 2) asteroids with primary metallic composition and secondary deposition of silicates from external sources; 3) analogs of bencubbinite meteorites; and 4) asteroids undergone smelting-like reactions in the presence of carbon at high temperatures.[198]

The thermal history of the M-type asteroids has been reviewed through the study of the iron meteorites by Goldstein et al.[201] who found some interesting conclusions: 1) cooling rates vary from 60°C to 300°C/Ma for the IIIAB group and 100°C–6600°C/Ma for the IVA group; 2) the IVA crystallized and cooled in a metallic body of 150 ± 50 km of radius with scarce or no silicate insulation; 3) the ungrouped irons come from 50 different parent bodies as large as 1000 km that may have undergone fractional crystallization and; 4) these parent bodies accreted even before the chondrites, possibly at 1–2 au of distance from the Sun <1 Ma after CAI, and then were scattered into the AB by protoplanets. High-precision W isotope measurements from 33 iron meteorites combined with parent body sizes into a model of planetesimal heating by ^{26}Al decay determined that accretion of the parent body occurred within 1.5 Ma after CAI.[162]

Mesosiderites, characterized by a 50-50% proportion of metal (iron and nickel) and silicates, had a different thermal history from the irons. Mesosiderites cooled from 10^{4}°C to 10^{5}°C/Ma in the temperature range 850°C–1150°C while below 500°C they cooled at <0.5°C/Ma; such a dramatic difference, coupled with an observed scarcity of olivine, can be explained by the formation of mesosiderites through fragmentation of a parent body 200–400 km in diameter and subsequent reaccretion into a larger and differentiated one with an excellent insulation provided by the reaccreted debris.[202]

IGNEOUS PROCESSES IN COMETS

Comets are small objects of typically ~5 km in radius (i.e.[203]) and, due to the similarity of their spectral shapes to those of the inner disk, are thought to be among the building blocks of our Solar System.[204] Amorphous olivine but also crystalline olivine, basically its Mg-rich end member forsterite (Mg_2SiO_4), was detected in the spectra of comets 1P/Halley,[205] 2P/Encke,[206] 4P/Faye,[207] Mueller1993a,[208] C/1995 O1 Hale-Bopp,[209] 9P/Tempel 1,[210] 10P/Tempel 2,[211] 17P/Holmes,[212] 19P/Borrelly,[207] 21P/Giacobini-Zinner,[213] C/1996 B2 (Hyakutake),[214] C/1999 T1 (McNaught-Hartley),[215] 29P/Schwassmann-Wachmann 1,[216] 49P/Arend-Rigaux,[211] 55P/Tempel-Tuttle,[217] C/2001 HT50 (LINEAR-NEAT),[206] C/2002 O4 (Hönig),[218] C/2002 X1 (NEAT),[218] C/2002 X5 (Kudo-Fujikawa),[218] 67P/Churyumov-Gerasimenko,[206,219] 69P/Taylor,[218] 73P/Schwassmann-Wachmann 3,[220] 103P/Hartley 2,[221] and 162P/Siding Spring,[222] in the interplanetary dust particles (IDPs) speculated as originating from the comet 26P/Grigg-Skjellerup,[223] and it was directly found as presolar grains of the comet 81P/Wild 2 returned to Earth by the Stardust mission.[3–5] However, there are also exceptions. For example, phyllosilicates and organics instead of olivine and pyroxenes were found in the comet P/2016 BA_{14} (PANSTARRS).[224] The distribution of these comets is quite heterogeneous, aside the Halley-type and Encke-type comets some of them belong to the Jupiter-family, others (i.e. P/2019 LD2[225]) are transiting from Centaur group to Jupiter-family, and others to the Oort cloud family, thus implying that the igneous processes producing the crystalline olivine were well distributed along the original places where the comets formed. This in the case that crystalline olivine is formed by thermal annealing of amorphous ferromagnesian silicate under vacuum at temperatures of 870 K–1020 K.[226] In such a case, if we want to understand whether the igneous processes that formed the olivine actually occurred in the original place of formation of the comets or not, it is very important to know where the comets and the olivine present in their nuclei formed. Various hypotheses for the origin of the so-called building blocks of

the Solar System exist, sometimes conflicting among them; it is thus important to explore them in order to find an eventual synthesis for a unifying hypothesis. Or, possibly, find different mechanisms for different places.

The formation of crystalline forsterite was thought to be occurring through thermal annealing of amorphous silicates within 1 au from the proto-Sun where the temperature was ~1000 K.[164,227] Actually, laboratory experiments of thermal annealing on amorphous ferromagnesian silicate under vacuum at temperatures of 870 K–1020 K produced pure forsterite crystals very similar to those found in glass with embedded metals and sulphides (GEMS) occurring in interplanetary dust particles (IDPs).[226] The process of thermal annealing close to the proto-Sun then requires a mechanism of transport of the processed crystals to the outer parts of the nebula where they could be incorporated in cometary nuclei.[228] Furthermore, just to add more complexity to an already complex problem, some of the observed GEMS display isotopic oxygen anomalies that suggest a clear pre-solar origin (i.e.[229]). Available models show how the transport of refractory materials produced in the hotter regions of the proto-nebula is a natural evolution leading to the formation of protoplanetary disks.[230] Protostellar jets and winds, commonly associated with forming stars, can cause melting of small inclusions even at several au of distance from the Sun and redistribute materials in the Solar System. The outward transport of the products may have occurred by both advection and gas-drag-driven radial drift in the protoplanetary nebula, which can overcome the inward drift produced by the proto-Sun, provided a weakly turbulent regime existed in the protoplanetary nebula, and thus delivery of the forsterite grains to the outer regions of the Solar System in 10^4[231] or in 10^6 years.[232] It is not yet certain whether a turbulent regime actually existed in the protoplanetary nebula but isotopic studies in five olivine particles found in comet 81P/Wild 2 support the case for the formation close to the proto-Sun with subsequent transport to the Kuiper Belt where the comet accreted.[233]

However, observations of the HD100546 star system showed how the mass fraction of crystalline silicates increases with decreasing temperatures at larger radial distances from the central star,[234,235] which is inconsistent with the process of formation by thermal annealing close to the proto-Sun. A possible explanation is the amorphization of crystalline silicate in the interstellar medium by heavy-ion cosmic radiation.[236–239] In such a case, despite the low abundance of forsterite grains in the interstellar medium,[240] the discovery of forsterite grains in cometary nuclei opens the possibility that such grains are interstellar relics entrained in our outer Solar System.[241] These grains show a significant enrichment in $^{18}O/^{16}O$ (13 times the solar value) and depletions in $^{17}O/^{16}O$ (one-third solar) and $^{29}Si/^{28}Si$ (<0.8 times solar), indicative of formation from a type II supernova.[242] This process requires that the accretion of most cometary nuclei occurred in the outermost Solar System or that the interstellar grains migrated deep into the outer Solar System from the interstellar space to be entrained in cometary nuclei. A study on the dynamical properties of comets having hyperbolic orbits concluded that those of interstellar origin have decreasing eccentricity and perihelion whereas those of Oort cloud origin have decreasing eccentricity and increasing perihelion; this study also concludes that both TSOs 1I/Oumuamua and 2I/Borisov are most likely comets of interstellar origin.[243] This observation would be somehow consistent with the process of cometary formation in the outer Solar System. However, it is the probability of being an interstellar object that increases with decreasing eccentricity and perihelion, which means that interstellar objects tend to have small eccentricities and perihelia while Oort cloud comets tend to have small eccentricities but large perihelia. The majority of the Halley-type comets originate from near parabolic flux within $q < 2$ au from the Sun in contrast to those of the Jupiter-family with initial perihelion beyond the orbit of Saturn,[244] although at varying distances from the Sun, both of which are still quite far away from the regions of the Solar System having direct access to the interstellar space. Lyttleton,[245] from the analysis of the distribution of the orbits of long period comets, noticed already in the late 60s that there is no basis for the existence of a shell of comets at great distance from the Sun. This study was in clear antithesis with the hypothesis of Oort[246] who postulated a region of formation for the comets located between 5×10^4 and 15×10^4 au from the Sun. Another study evidenced how a massive hypothetical planet 9 (HP9) located between 200 and 400 au from the Sun may cause transitions from a hyperbolic to a parabolic orbit in comets and vice versa.[247] Batygin and Brown's[248] calculations suggested a planet >10 Earth masses at 700 au of distance from the Sun "to produce the desired effect" and to explain the presence of high-perihelion Sedna-like objects. Depending on the evolution of the gas disk, such a massive HP9 could have perihelion between 300 and 1500 au.[249] Trujillo and Sheppard[250] indeed found another Sedna-like object at 80 au of perihelion confirming that Sedna is not an isolated object in the TS and that could be a link between KBOs and IOC objects.

A last possibility suggested by laboratory experiments is that magnesium silicide produced in the hydrogen-rich gas outflow of evolved stars might have been incorporated in the protoplanetary nebula where it would have been easily turned into forsterite through oxidation with the relatively oxygen-rich solar gas; if a significant fraction of the forsterite observed in our Solar System was produced through this reaction, it could explain the lower abundance of forsterite in presolar grains and its variable distribution along the Solar System.[251]

CHRONOLOGICAL SEQUENCE OF HEATING PROCESSES AND KEY FORMATION EVENTS

Although chondrule formation is a localized phenomenon, the analysis of grains found in primitive meteorites, asteroids, and comets, evidenced large-scale heating events in the solar nebula that can be considered as the first igneous processes in our Solar System.[252] From the observation of T Tauri stars and from isotopic data, it is inferred that the persistence of the protoplanetary disk lasted for 10^7 years.[253] Chemical zoning patterns in metallic grains (iron, nickel) found in CC imply formation at very low pressure ($\sim10^{-4}$ bar) with temperatures between 1270 K and 1370 K and subsequent condensation at a cooling rate of $\sim$0.2 K h^{-1}.[252] CAI crystallized at temperatures between 1700 K and 1800 K at cooling rates between 2 and 50 K/h^{-1}.[254] Due to the high melting temperature of olivine (2,163 $\pm$ 25 K[255]), some AOAs have never been melted and have probably undergone only moderate thermal annealing close to the proto-Sun[104,256] thus representing the earliest condensates of the protoplanetary disk[257] together with CAIs.[258] Condensation of forsterite occurs at 1,370 K in a low pressure (10^{-4} bar) nebular environment of solar composition.[259] AOAs, consisting predominantly of forsterite, formed in a similar environment (10^{-6}–10^{-4} bar) over a range of temperatures between 1200 K and 1384 K.[260] AOAs were found in presolar grains that survived every kind of processing both in the interstellar space and in the solar nebula whereas all the other materials were heated and then homogenized to an average composition.[261–263]

According to U-corrected-Pb-Pb chronology, AOAs and CAIs have an absolute age of 4567.3 $\pm$ 0.16 Ma (another measurement in NWA 2364 points to 4,568.2 Ma for CAIs[37]) and were formed by evaporation, condensation, and aggregation in a >1300 K hot gas of solar composition close to the proto-Sun; subsequently, some CAIs were melted both inside and outside their region of formation by still unknown transient heating events.[258] Hu et al.[264] speculate that such transient heating events might be related to rapid solar outbursts when the proto-Sun went through EXor or FUor phases, named from the pre-main-sequence stars EX Lupi and FU Orionis, which are characterized by episodic brightness and quiescent periods.[265] FU Orionis events occur in a timescale of 100 years whereas EX Lupi in 1 year.[266] Marrocchi et al.[257] reconstructed a possible timeline for the evaporation, condensation, and aggregation processes that characterized the AOAs formation: 1) condensation may have occurred from days to weeks after the evaporation; 2) aggregation around a year after condensation; 3) thermal annealing more than decades after the aggregation. These processes occurred after CAI formation. Then, after AOAs follows chondrule formation, it is generally inferred that chondrules formed 1–1.5 Ma after CAI.[267] A different timeline for thermal annealing was proposed by Krot et al.,[268] although maintaining the same sequence of events: days to weeks of thermal annealing at 1,373 K with slow cooling rates ($\sim$0.01 K h^{-1}); formation of chondrules 5 Ma after CAI. ^{26}Mg content of CAIs found in Acfer 094 showed that they formed under canonical $^{26}Al/^{27}Al$ ratio of 5×10^{-5} in $\sim$300,000 years; four CAIs showed a poor content of ^{26}Mg thus suggesting that probably they never contained ^{26}Al.[269] Other data suggest that CAIs and chondrules formed almost at the same age (4,567.30 Ma and 4,567.32–4,564.71 Ma, respectively) but, at the end, the range given for chondrules formation corresponds to $\sim$2.61 Ma.[270] As it could be seen for the formation of the chondrules, there is a variety of ages in the literature of planetary accretion that it would be simply too long to be completely listed here. Just as an example, in some models, Jupiter could be accreted as fast as 3 Ma,[53,271] and the Earth as slow as 30–40 Ma,[272] although slower accretion times would be expected at increasing distance from the Sun (i.e.[273]). An average duration of key events of formation in our Solar System, along with a range of temperatures, is given in Table 1 and shown in Figure 1.

DISCUSSION

Although there are still uncertainties when we push toward our observational limits, the high amount of information now available allows us to understand that igneous processes in our Solar System could be as ancient as its origin and that the AOAs found in presolar grains could be even older than the Solar System itself. Their presence is ubiquitous and pervasive, they were found in almost every type of small body of the Solar System, and their initial origin is still uncertain. It is not clear whether they formed within our Solar System, or came in it from outside, or both as far as we know. At the moment, the analysis of the dwarf

Table 1. Duration time and temperature of key formation events in our Solar System assuming a total duration of 10^7 years for the persistence of the protoplanetary disk in our solar nebula

Event	Temperature (K)	Duration time (years)
Formation of the proto-Sun	10,000,000 Preibisch and Feigelson[285]	~950,000 Wuchterl and Klessen[286]
Formation of CAIs	1,800–1,700 Stolper and Paque[254]	~300,000 Sugiura and Krot[269]
Formation of AOAs	1,384–1,200 Ruzicka et al.[260]	~100 Marrocchi et al.[257]
Formation of planetesimals	1,598–1888 Kaminski et al.[287]	~1,000,000 Kruijer et al.; Chambers[65,288]
Formation of chondrules	1,370 Sugiura et al.[259]	~2,000,000 Pape et al.[289]
Formation of the proto-Earth	4,700–5,000 Sasaki and Nakazawa; Canup[290,291]	~5,000,000 Nakagawa et al.[273]
Formation of TNOs	450–675 Malamud et al.[292]	~10,000,000 Kenyon and Bromley[293]

The duration time of the various events must be counted from the formation of the proto-Sun.

planets is not of much help to understand the origin of the olivine found in some of them because little is still known about them despite the Dawn mission to Ceres and New Horizons to the Pluto system. Although the modeling of serpentinization of a rocky core for Charon and the detection of serpentine on Ceres may suggest the presence of olivine and sufficient internal heat to favor the process of serpentinization, it seems that lava flows are not present and olivine was not detected on their surfaces. Even possible cryovolcanic processes show some elements of ambiguity both on Ceres and Charon, including the presence of mountains of poorly understood origin. The altered olivine (i.e. serpentine) that was found on Ceres might likely be the result of igneous processes in aqueous environment thus suggesting that some internal thermal activity was present in its past, perhaps even volcanic processes like those occurred on 4 Vesta, but more observations and studies are necessary before reaching a definitive conclusion. Similar processes may have occurred on the other dwarf planets Haumea and Sedna where serpentinization was postulated to match the available spectra. Again, more dedicated observation would be needed as well as for the other dwarf planets beyond the Pluto orbit not yet reached by a spacecraft.

Asteroids and comets are more promising, also given past and ongoing sample return missions that found crystalline olivine on Bennu, Itokawa, P81/Wild 2, and the huge collections of available meteorites found on Earth. AOAs found in Murchison meteorite are fine-grained, grain size is around 2 μm, and show several triple junctions thus suggesting episodes of sintering after the aggregation.[259] This observation may lead us to think that AOAs might perhaps be the result of various episodes of recycling of nebular condensates, a similar conclusion drawn by Marrocchi et al.[274] AOAs found in the Kainsaz CO3.2 chondrite show thermal metamorphism suggesting that their formation occurred during a fluid-driven process at < 500°C (~773 K) in its parent body.[275] Probably, AOAs were already present within the parent body since the time of its accretion and then they were subject to thermal metamorphism afterward, it could be a plausible explanation given that primordial igneous processes in asteroidal parent bodies are not so uncommon. The initial processes of star formation may shed some light on the origin of AOAs that were present in the nebular dust from which our Solar System formed. Dauphas and Chaussidon[276] described this process, which is quoted as follows with the most interesting part highlighted in italic font: ''During collapse of the solar system's parent molecular cloud core, conservation of angular momentum led to the formation of a protoplanetary disk (or proplyd), through which material accreted by the Sun was channeled. In the inner part of the disk, most material was condensed from cooling gas of near-solar composition (Grossman 1972, Grossman & Larimer 1974). *The dust particles thus created, as well as those inherited from the parent molecular cloud (0.1–10 μm)*, are thought to have aggregated by Brownian motion, differential vertical settling, and turbulence …''. Therefore, this sentence in italic might be interpreted as the AOAs were already present in the nebular dust well before the formation of the central star. This means that AOAs might also be the result of recycling of previously existing grains that escaped reprocessing at star temperatures or above the melting point of forsterite. Maybe these grains were reprocessed in a previous star formation, difficult to say with certainty, but the point is that the age inferred from the petrologic history of the oldest grains found so far in NWA 2364 (4,368.2 Ma) corresponds to the proto-Sun formation age at the earliest. Similar origin close to the proto-Sun at a temperature of ~1000 K was postulated for the T77/F50 sample found in comet 81P/Wild 2,[233] although an explicit age was not said. Nevertheless, nothing older than these samples has been found yet thus implying that recycled grains from the parent molecular cloud were not found yet. But yet mixtures of olivine and pyroxenes match the spectral properties of the interstellar dust observed in the Milky Way (i.e.[277]).

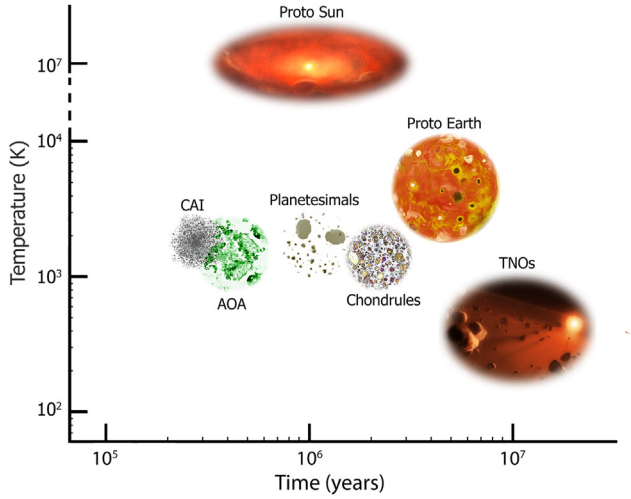

Figure 1. Time vs. temperature diagram showing the sequence of events occurred in the early Solar System
The temperature axis has been shortened (dotted line) for graphical reasons, the proto-Sun would be far out of the figure.

A heterogeneous distribution of long-lived radiogenic elements all over the Solar System may explain the current presence of ^{238}U fueling the Earth's volcanic activity and the active cryo-volcanism of Enceladus[278] whereas such activity is now extinct in other bodies of the inner and outer Solar System. However, as already mentioned in section Distribution of PHS in the Solar System's protoplanetary disk, many lines of evidence point to a widespread and homogeneous distribution of ^{26}Al in the galaxy and in our Solar System as well.[35–37] An obvious implication of such a widespread distribution is that early heating processes affected almost every small (and large) body of the Solar System in which ^{26}Al was present. Among the short-lived radiogenic elements, now extinct, ^{26}Al was the dominant source overwhelming the long-lived radiogenic elements (i.e.[279]). The consequence is that the early Solar System experienced intense but relatively short (in time) igneous processes when compared to those fueled by long-lived radiogenic elements. But the long-period volcanic processes, either hot or cold, could only occur in those bodies where long-lived radiogenic elements like ^{238}U, for example, were present since their accretion, which is the case of the Earth, possibly Venus (if confirmed), and Enceladus. All the other bodies had volcanism as long as their residual internal heat, and/or a possibly limited abundance of long-lived radiogenic elements, allowed it. Their geologic activity ceased once their radiogenic sources became extinct unless kept alive by tidal heating processes, which is the case of Io and only partially of Enceladus. Thus, the ending time of volcanic processes depends on the initial abundance of long-lived radiogenic elements that each body acquired from the protoplanetary disk during its accretion. This abundance obviously depends on the distribution of the long-lived radiogenic elements in the solar nebula.

APPLICATION OF GALACTIC COSMIC RAYS (GCR) TO THE STUDIES OF THE SMALL BODIES OF THE SOLAR SYSTEM

Given the importance of the density for the compositional and geophysical characterization of the small bodies of the Solar System (SBSS) seen throughout this review, as density is a diagnostic parameter for the characterization of magma composition, we will briefly introduce here the possibilities of application of the GCR to the SBSS to characterize the density through a methodology called "muography". Similar to X-ray technology, muography takes advantage of the strong penetration of cosmic-ray atmospheric muons (high-energy muons generated in the Earth's atmosphere can travel through 1 km or more on rock before decaying), to image the internal structure of gigantic geological and manmade objects on land (e.g., volcanoes, for instance in the study by Leone et al.[280] and pyramids, for instance in the study by Morishima et al.[281]) and also in the ocean (e.g., tsunami in the study by Tanaka et al.[282]). Due to the penetration power of high-energy muons, they can travel through liquid and solid targets; therefore, it is possible to create images with this method (similar to X-ray photographs) to directly measure the density distribution in the SBSS.

However, unlike on Earth, since SBSS do not have their own atmosphere, GCR directly interact with the solid materials of SBSS. Prettyman[283] combined the Fluktuierende Kaskade Monte Carlo simulations in "standard rock" with $Z = 11$, $A = 22$, approximately $(FeO)_{0.2}(SiO_2)_{0.8}$ with the cascade model proposed by Gaisser et al.[284] and found the following relationship between the muon flux and the density of solid materials:

$$\Phi(E\mu > 1\ GeV) = 10^{-0.7\ log(\rho)-3} muons\ cm^{-2} s^{-1} sr^{-1}$$

The production of muons decreases sharply as the density of the production target increases. For example, while ~8 muons m^{-2} s^{-1} sr^{-1} are generated in SiO_2 with a density of 2 g cm^{-2}, the flux of muons generated in materials with iron-nickel composition (ρ= 8 g cm^{-3}) would be ~2 muons m^{-2} s^{-1} sr^{-1}. As a result, while the muon flux at 1 GeV is almost the same in the open-sky vertical muon flux on Earth, the flux at 100 GeV is more than 3 order of magnitude smaller on asteroids than on Earth. Based on this result, we can conclude that it is unpractical to target with muography an SBSS with a diameter larger than 100 m where the bulk density would be assumed to match the density of the asteroid 101955 Bennu (~1.2 g cm^{-3}).

CONCLUSIONS

The picture that we draw from all this information is that igneous processes in the Solar System can be distinguished in two main types in terms of duration: short-period (Ma timescale) and long-period (Ga timescale). Short-period igneous processes are those related to the early phases of the formation of the Solar System, from the proto-Sun formation to the extinction of the short-lived radiogenic elements; long-period igneous processes are those following the end of the short-lived radiogenic elements and thus fueled by the long-lived radiogenic elements only. Short-period igneous processes were brief but intense, forming magma oceans in those planetary bodies richer in ^{26}Al, whereas long-period igneous processes are longer and less intense but still maintain geologic activity on Earth, possibly Venus, and Enceladus. The key findings of this review can be resumed as follows:

- The distribution of the PHS fueling short-period igneous processes was widespread all over the protoplanetary disk whereas those fueling long-period igneous processes were not widespread and limited only to the regions of the disk where active bodies are observed today. In this regard, we conclude that the absence of igneous processes in the asteroids of the Watsonia family might just be an exception.
- Thermal metamorphism has been postulated on various bodies, including dwarf planets, thus implying that it might likely be related to the short-period igneous processes given the evident absence of long-period igneous processes. However, long-period igneous processes now extinct cannot be totally excluded.
- The distribution of AOAs is also widespread, the presence of both amorphous and crystalline olivine was found in a wide range of comets (both short-period and long-period), thus suggesting both internal origin within our Solar System and external entrainment from interstellar space. This explanation does not require very long transport processes of the AOAs from the Sun to the most extreme regions of the outer Solar System and, also important, volcanic processes for their formation.
- Finding olivine or not on the surfaces of dwarf planets will not change the conclusion drawn on the basis of the wide distribution of the comets. If present, olivine should be among the densest parts in the composition of the dwarf planets, thus likely sunk in their most internal rocky layers, which could hardly make it to the surface unless expelled as dust entrained in water vapor and then redeposited by cryovolcanic processes. In such a case, it would be the only chance to detect it on the surface.
- AOAs and CAIs close ages show that they formed almost at the same time with the important difference that CAIs surely formed within the protoplanetary disk of our Solar System whereas AOAs might have also been formed in previously existing nebular processes older than our Solar System.
- The unexpected lack of chondrules in samples returned from 162173 Ryugu, coupled to the statistics of meteorite falls on Earth, suggests that they might have been overestimated and thus be uncommon. This finding is certainly interesting but more observation is needed to draw a definitive conclusion.

- Muography could be a useful tool in assessing the density of the asteroids, provided their diameters are <100 m.

Finally, we found that the average bulk density is an important parameter to estimate the composition of a body and thus any improvement in the measurements would be welcome. Muography can certainly improve density measurements where its application in space would be possible.

We have made another step forward in understanding the possible origin of the igneous processes and of the building blocks of the Solar System. However, the road is still long and will likely lead to the study of other observable star systems in which we may find similarities or differences that will be statistically significant to better understand if our Solar System and the igneous processes in it are common or uncommon.

ACKNOWLEDGMENTS

The authors are grateful to Daniele Gasparri for the figure.

AUTHOR CONTRIBUTIONS

"G.L. and H.K.M.T. conceived, designed the study, drafted and reviewed the manuscript. Both authors read and approved the manuscript".

DECLARATION OF INTERESTS

The authors declare no competing interests.

REFERENCES

1. Mcsween, H.Y. (1989). Achondrites and igneous processes on asteroids. Annu. Rev. Earth Planet. Sci. *17*, 119–140.

2. Wilson, L., and Keil, K. (2012). Volcanic activity on differentiated asteroids: A review and analysis. Chem. Erde *72*, 289–321. https://doi.org/10.1016/J.CHEMER.2012.09.002.

3. Brownlee, D. (2014). The Stardust Mission: Analyzing Samples from the Edge of the Solar System. Nat. Astron. *42*, 179–205. https://doi.org/10.1146/ANNUREV-EARTH-050212-124203.

4. Zolensky, M.E., Zega, T.J., Yano, H., Wirick, S., Westphal, A.J., Weisberg, M.K., Weber, I., Warren, J.L., Velbel, M.A., Tsuchiyama, A., et al. (2006). Mineralogy and petrology of comet 81P/wild 2 nucleus samples. Science *314*, 1735–1739. https://doi.org/10.1126/SCIENCE.1135842.

5. Leroux, H., Jacob, D., Stodolna, J., Nakamura-Messenger, K., and Zolensky, M.E. (2008). Igneous Ca-rich pyroxene in comet 81P/Wild 2. Am. Mineral. *93*, 1933–1936. https://doi.org/10.2138/AM.2008.3048.

6. Scott, E.R. (2007). Chondrites and the Protoplanetary Disk. Annu. Rev. Earth Planet. Sci. *35*, 577–620. https://doi.org/10.1146/annurev.earth.35.031306.140100.

7. Saji, N.S., Wielandt, D., Holst, J.C., and Bizzarro, M. (2020). Solar system Nd isotope heterogeneity: Insights into nucleosynthetic components and protoplanetary disk evolution. Geochim. Cosmochim. Acta *281*, 135–148. https://doi.org/10.1016/J.GCA.2020.05.006.

8. Ikoma, M., Elkins-Tanton, L., Hamano, K., and Suckale, J. (2018). Water Partitioning in Planetary Embryos and Protoplanets with Magma Oceans. Space Sci. Rev. *214*, 76. https://doi.org/10.1007/S11214-018-0508-3.

9. Keil, K., Stöffler, D., Love, S.G., and Scott, E.R.D. (1997). Constraints on the role of impact heating and melting in asteroids. Meteorit. Planet. Sci. *32*, 349–363. https://doi.org/10.1111/J.1945-5100.1997.TB01278.X.

10. Love, S.G., and Ahrens, T.J. (1996). Catastrophic Impacts on Gravity Dominated Asteroids. Icarus *124*, 141–155. https://doi.org/10.1006/ICAR.1996.0195.

11. Brauer, F., Henning, T., and Dullemond, C.P. (2008). Planetesimal formation near the snow line in MRI-driven turbulent protoplanetary disks. Astron. Astrophys. *487*, L1. https://doi.org/10.1051/0004-6361:200809780.

12. Jansson, K.W., Johansen, A., Syed, M.B., and Blum, J. (2017). The role of pebble fragmentation in planetesimal formation. ii. numerical simulations. Astrophys. J. *835*, 109. https://doi.org/10.3847/1538-4357/835/1/109.

13. Jura, M., Xu, S., and Young, E.D. (2013). 26Al in the early solar system: not so unusual after all. Astrophys. J. *775*, L41. https://doi.org/10.1088/2041-8205/775/2/L41.

14. Shukolyukov, A., and Lugmair, G.W. (1993). Live Iron-60 in the Early Solar System. Science *259*, 1138–1142. https://doi.org/10.1126/SCIENCE.259.5098.1138.

15. Wielandt, D., Nagashima, K., Krot, A.N., Huss, G.R., Ivanova, M.A., and Bizzarro, M. (2012). Evidence for multiple sources of 10Be in the early solar system. Astrophys. J. *748*, L25. https://doi.org/10.1088/2041-8205/748/2/L25.

16. Weissman, P.R. (1990). The Oort cloud. Nature *344*, 825–830. https://doi.org/10.1038/344825a0.

17. Gladman, B., and Volk, K. (2021). Transneptunian Space. Annu. Rev. Astron. Astrophys. *59*, 203–246. https://doi.org/10.1146/annurev-astro-120920-010005.

18. Duncan, M., Quinn, T., and Tremaine, S. (1987). The formation and extent of the solar system comet cloud. Astron. J. *94*, 1330–1338.

19. Baxter, E.J., Blake, C.H., and Jain, B. (2018). Probing Oort Clouds around Milky Way Stars with CMB Surveys. Astron. J. *156*, 243. https://doi.org/10.3847/1538-3881/AAE64E.

20. Shannon, A., Jackson, A.P., Veras, D., and Wyatt, M. (2015). Eight billion asteroids in the Oort cloud. Mon. Not. R. Astron. Soc. *446*, 2059–2064. https://doi.org/10.1093/MNRAS/STU2267.

21. Correa-Otto, J.A., and Calandra, M.F. (2019). Stability in the most external region of the Oort Cloud: evolution of the ejected comets. Mon. Not. R. Astron. Soc. *490*, 2495–2506. https://doi.org/10.1093/MNRAS/STZ2671.

22. Torres, S., Cai, M.X., Brown, A.G.A., and Zwart, S.P. (2019). Galactic tide and local stellar perturbations on the Oort

cloud: creation of interstellar comets. Astron. Astrophys. *629*, A139. https://doi.org/10.1051/0004-6361/201935330.

23. Gladman, B., Kavelaars, J.J., Petit, J.-M., Morbidelli, A., Holman, M.J., and Loredo, T. (2001). The Structure of the Kuiper Belt: Size Distribution and Radial Extent. Astron. J. *122*, 1051–1066. https://doi.org/10.1086/322080.

24. Schrader, D.L., Nagashima, K., Krot, A.N., Ogliore, R.C., Yin, Q.Z., Amelin, Y., Stirling, C.H., and Kaltenbach, A. (2017). Distribution of 26Al in the CR chondrite chondrule-forming region of the protoplanetary disk. Geochim. Cosmochim. Acta *201*, 275–302. https://doi.org/10.1016/J.GCA.2016.06.023.

25. Bizzarro, M., Connelly, J.N., and Krot, A.N. (2017). Chondrules: Ubiquitous Chondritic Solids Tracking the Evolution of the Solar Protoplanetary Disk. In Formation, Evolution, and Dynamics of Young Solar Systems. Astrophysics and Space Science Library, *445*, M. Pessah and O. Gressel, eds (Springer), pp. 161–195. https://doi.org/10.1007/978-3-319-60609-5_6.

26. Larsen, K.K., Trinquier, A., Paton, C., Schiller, M., Wielandt, D., Ivanova, M.A., Connelly, J.N., Nordlund, Å., Krot, A.N., and Bizzarro, M. (2011). Evidence for magnesium isotope heterogeneity in the solar protoplanetary disk. Astrophys. J. *735*, L37. https://doi.org/10.1088/2041-8205/735/2/L37.

27. Krot, A.N., Makide, K., Nagashima, K., Huss, G.R., Ogliore, R.C., Ciesla, F.J., Yang, L., Hellebrand, E., and Gaidos, E. (2012). Heterogeneous distribution of 26Al at the birth of the solar system: Evidence from refractory grains and inclusions. Meteorit. Planet. Sci. *47*, 1948–1979. https://doi.org/10.1111/MAPS.12008.

28. Ku, Y., and Jacobsen, S.B. (2020). Potassium isotope anomalies in meteorites inherited from the protosolar molecular cloud. Sci. Adv. *6*, eabd0511. https://doi.org/10.1126/SCIADV.ABD0511.

29. Tang, H., and Dauphas, N. (2012). Abundance, distribution, and origin of 60Fe in the solar protoplanetary disk. Earth Planet. Sci. Lett. *359–360*, 248–263. https://doi.org/10.1016/J.EPSL.2012.10.011.

30. Thrane, K., Bizzarro, M., and Baker, J.A. (2006). Extremely Brief Formation Interval for Refractory Inclusions and Uniform Distribution of 26 Al in the Early Solar System. Astrophys. J. *646*, L159–L162. https://doi.org/10.1086/506910.

31. Kita, N.T., Yin, Q.Z., Macpherson, G.J., Ushikubo, T., Jacobsen, B., Nagashima, K., Kurahashi, E., Krot, A.N., and Jacobsen, S.B. (2013). 26Al-26Mg isotope systematics of the first solids in the early solar system. Meteorit. Planet. Sci. *48*, 1383–1400. https://doi.org/10.1111/MAPS.12141.

32. Ushikubo, T., and Kimura, M. (2021). Oxygen-isotope systematics of chondrules and olivine fragments from Tagish Lake C2 chondrite: Implications of chondrule-forming regions in protoplanetary disk. Geochim. Cosmochim. Acta *293*, 328–343. https://doi.org/10.1016/J.GCA.2020.11.003.

33. Mishra, R.K., and Chaussidon, M. (2014). Timing and extent of Mg and Al isotopic homogenization in the early inner Solar System. Earth Planet. Sci. Lett. *390*, 318–326. https://doi.org/10.1016/J.EPSL.2013.12.042.

34. Gregory, T., Luu, T.H., Coath, C.D., Russell, S.S., and Elliott, T. (2020). Primordial formation of major silicates in a protoplanetary disc with homogeneous 26Al/27Al. Sci. Adv. *6*, 9626–9637. https://doi.org/10.1126/SCIADV.AAY9626.

35. Mahoney, W.A., Ling, J.C., Wheaton, W.A., Jacobson, A.S., Mahoney, W.A., Ling, J.C., Wheaton, W.A., and Jacobson, A.S. (1984). HEAO 3 discovery of Al-26 in the interstellar medium. ApJ *286*, 578–585. https://doi.org/10.1086/162632.

36. Russell, S.S., Srinivasan, G., Huss, G.R., Wasserburg, G.J., and MacPherson, G.J. (1996). Evidence for Widespread 26Al in the Solar Nebula and Constraints for Nebula Time Scales. Science *273*, 757–762. https://doi.org/10.1126/SCIENCE.273.5276.757.

37. Bouvier, A., and Wadhwa, M. (2010). The age of the Solar System redefined by the oldest Pb–Pb age of a meteoritic inclusion. Nat. Geosci. *3*, 637–641. https://doi.org/10.1038/ngeo941.

38. Rubin, A.E. (2000). Petrologic, geochemical and experimental constraints on models of chondrule formation. Earth Sci. Rev. *50*, 3–27. https://doi.org/10.1016/S0012-8252(99)00067-7.

39. Herbst, W., Greenwood, J.P., and Yap, T.E. (2021). The Macroporosity of Rubble Pile Asteroid Ryugu and Implications for the Origin of Chondrules. Planet. Sci. J. *2*, 110. https://doi.org/10.3847/PSJ/ABF7C0.

40. Amelin, Y., and Ireland, T.R. (2013). Dating the Oldest Rocks and Minerals in the Solar System. Elements *9*, 39–44. https://doi.org/10.2113/GSELEMENTS.9.1.39.

41. Amelin, Y., Krot, A.N., Hutcheon, I.D., and Ulyanov, A.A. (2002). Lead isotopic ages of chondrules and calcium-aluminum-rich inclusions. Science *297*, 1678–1683. https://doi.org/10.1126/science.1073950.

42. Connelly, J.N., Bizzarro, M., Krot, A.N., Nordlund, Å., Wielandt, D., and Ivanova, M.A. (2012). The Absolute Chronology and Thermal Processing of Solids in the Solar Protoplanetary Disk. Science *338*, 651–655. https://doi.org/10.1126/SCIENCE.1226919.

43. Bollard, J., Connelly, J.N., Whitehouse, M.J., Pringle, E.A., Bonal, L., Jørgensen, J.K., Nordlund, Å., Moynier, F., and Bizzarro, M. (2017). Early formation of planetary building blocks inferred from Pb isotopic ages of chondrules. Sci. Adv. *3*, e1700407. https://doi.org/10.1126/SCIADV.1700407.

44. Lissauer, J.J. (1987). Timescales for planetary accretion and the structure of the protoplanetary disk. Icarus *69*, 249–265. https://doi.org/10.1016/0019-1035(87)90104-7.

45. Weidenschilling, S.J. (2008). Accretion of planetary embryos in the inner and outer solar system. Phys. Scr. *2008*, 014021. https://doi.org/10.1088/0031-8949/2008/T130/014021.

46. Morbidelli, A., Lunine, J.I., O'Brien, D.P., Raymond, S.N., and Walsh, K.J. (2012). Building Terrestrial Planets. Annu. Rev. Earth Planet. Sci. *40*, 251–275. https://doi.org/10.1146/ANNUREV-EARTH-042711-105319.

47. Leone, G., Tackley, P.J., Gerya, T.V., May, D.A., and Zhu, G. (2014). Three-dimensional simulations of the southern polar giant impact hypothesis for the origin of the martian dichotomy. Geophys. Res. Lett. *41*, 8736–8743. https://doi.org/10.1002/2014GL062261.

48. Leone, G. (2016). Alignments of volcanic features in the southern hemisphere of Mars produced by migrating mantle plumes. J. Volcanol. Geotherm. Res. *309*, 78–95. https://doi.org/10.1016/j.jvolgeores.2015.10.028.

49. Thiemens, M.M., Sprung, P., Fonseca, R.O.C., Leitzke, F.P., and Münker, C. (2019). Early Moon formation inferred from hafnium–tungsten systematics. Nat. Geosci. *12*, 696–700. https://doi.org/10.1038/s41561-019-0398-3.

50. Morbidelli, A., Lambrechts, M., Jacobson, S., and Bitsch, B. (2015). The great dichotomy of the Solar System: Small terrestrial embryos and massive giant planet cores. Icarus *258*, 418–429. https://doi.org/10.1016/J.ICARUS.2015.06.003.

51. Lambrechts, M., Morbidelli, A., Jacobson, S.A., Johansen, A., Bitsch, B., Izidoro, A., and Raymond, S.N. (2019). Formation of planetary systems by pebble accretion and migration - How the radial pebble flux determines a terrestrial-planet or super-Earth growth mode. Astron. Astrophys. *627*, A83. https://doi.org/10.1051/0004-6361/201834229.

52. Bitsch, B., Izidoro, A., Johansen, A., Raymond, S.N., Morbidelli, A., Lambrechts, M., and Jacobson, S.A. (2019). Formation of planetary systems by pebble accretion and migration: growth of gas giants. Astron. Astrophys. *623*, A88. https://doi.org/10.1051/0004-6361/201834489.

53. Alibert, Y., Venturini, J., Helled, R., Ataiee, S., Burn, R., Senecal, L., Benz, W., Mayer, L., Mordasini, C., Quanz, S.P., et al. (2018). The formation of Jupiter by hybrid pebble–planetesimal accretion. Nat. Astron. *2*, 873–877. https://doi.org/10.1038/s41550-018-0557-2.

54. Ormel, C.W., and Ormel, C.W. (2017). The Emerging Paradigm of Pebble Accretion. In Formation, Evolution, and Dynamics of Young Solar Systems (Springer), pp. 197–228. https://doi.org/10.1007/978-3-319-60609-5_7.

55. Ida, S., Yamamura, T., and Okuzumi, S. (2019). Water delivery by pebble accretion to rocky planets in habitable zones in evolving disks. Astron. Astrophys. *624*, A28. https://doi.org/10.1051/0004-6361/201834556.

56. Morbidelli, A. (2020). Planet formation by pebble accretion in ringed disks. Astron. Astrophys. *638*, A1. https://doi.org/10.1051/0004-6361/202037983.

57. Mezger, K., Schönbächler, M., and Bouvier, A. (2020). Accretion of the Earth—Missing Components? Space Sci. Rev. *216*, 1–24. https://doi.org/10.1007/S11214-020-00649-Y.

58. Wänke, H., and Dreibus, G. (1988). Chemical composition and accretion history of terrestrial planets. Philos. Trans. R. Soc. London. Ser. A Math. Phys. Sci. *325*, 545–557.

59. Wänke, H., and Dreibus, G. (1994). Chemistry and accretion history of Mars. Philos. Trans. R. Soc. London. Ser. A Phys. Eng. Sci. *349*, 285–293. https://doi.org/10.1098/rsta.1994.0132.

60. Rubie, D.C., Frost, D.J., Mann, U., Asahara, Y., Nimmo, F., Tsuno, K., Kegler, P., Holzheid, A., and Palme, H. (2011). Heterogeneous accretion, composition and core–mantle differentiation of the Earth. Earth Planet. Sci. Lett. *301*, 31–42. https://doi.org/10.1016/J.EPSL.2010.11.030.

61. Fitoussi, C., Bourdon, B., and Wang, X. (2016). The building blocks of Earth and Mars: A close genetic link. Earth Planet. Sci. Lett. *434*, 151–160. https://doi.org/10.1016/J.EPSL.2015.11.036.

62. Liebske, C., and Khan, A. (2019). On the principal building blocks of Mars and Earth. Icarus *322*, 121–134. https://doi.org/10.1016/J.ICARUS.2019.01.014.

63. Kleine, T., Mezger, K., Münker, C., Palme, H., and Bischoff, A. (2004). 182Hf-182W isotope systematics of chondrites, eucrites, and martian meteorites: Chronology of core formation and early mantle differentiation in Vesta and Mars. Geochim. Cosmochim. Acta *68*, 2935–2946. https://doi.org/10.1016/j.gca.2004.01.009.

64. Kleine, T., Mezger, K., Palme, H., Scherer, E., and Münker, C. (2005). Early core formation in asteroids and late accretion of chondrite parent bodies: Evidence from 182Hf-182W in CAIs, metal-rich chondrites, and iron meteorites. Geochim. Cosmochim. Acta *69*, 5805–5818. https://doi.org/10.1016/J.GCA.2005.07.012.

65. Kruijer, T.S., Touboul, M., Fischer-Gödde, M., Bermingham, K.R., Walker, R.J., and Kleine, T. (2014). Protracted core formation and rapid accretion of protoplanets. Science *344*, 1150–1154. https://doi.org/10.1126/SCIENCE.1251766.

66. Lichtenberg, T., Dra Żkowska, J., Schönbächler, M., Golabek, G.J., and Hands, T.O. (2021). Bifurcation of planetary building blocks during Solar System formation. Science *371*, 365–370. https://doi.org/10.1126/science.abb3091.

67. Warren, P.H. (2011). Stable-isotopic anomalies and the accretionary assemblage of the Earth and Mars: A subordinate role for carbonaceous chondrites. Earth Planet. Sci. Lett. *311*, 93–100. https://doi.org/10.1016/J.EPSL.2011.08.047.

68. Kruijer, T.S., Burkhardt, C., Budde, G., and Kleine, T. (2017). Age of Jupiter inferred from the distinct genetics and formation times of meteorites. Proc. Natl. Acad. Sci. *114*, 6712–6716. https://doi.org/10.1073/pnas.1704461114.

69. Bollard, J., Kawasaki, N., Sakamoto, N., Olsen, M., Itoh, S., Larsen, K., Wielandt, D., Schiller, M., Connelly, J.N., Yurimoto, H., et al. (2019). Combined U-corrected Pb-Pb dating and 26Al-26Mg systematics of individual chondrules – Evidence for a reduced initial abundance of 26Al amongst inner Solar System chondrules. Geochim. Cosmochim. Acta *260*, 62–83. https://doi.org/10.1016/J.GCA.2019.06.025.

70. Kleine, T., Budde, G., Burkhardt, C., Kruijer, T.S., Worsham, E.A., Morbidelli, A., and Nimmo, F. (2020). The Non-carbonaceous–Carbonaceous Meteorite Dichotomy. Space Sci. Rev. *216*, 55. https://doi.org/10.1007/S11214-020-00675-W.

71. Kruijer, T.S., Kleine, T., and Borg, L.E. (2019). The great isotopic dichotomy of the early Solar System. Nat. Astron. *4*, 32–40. https://doi.org/10.1038/S41550-019-0959-9.

72. Kadlag, Y., Hirtz, J., Becker, H., Leya, I., and Mezger, K. (2021). Early solar irradiation as a source of the inner solar system chromium isotopic heterogeneity. Meteorit. Planet. Sci. *56*, 2083–2102. https://doi.org/10.1111/MAPS.13756.

73. Castillo-Rogez, J.C., Johnson, T.V., Thomas, P.C., Choukroun, M., Matson, D.L., and Lunine, J.I. (2012). Geophysical evolution of Saturn's satellite Phoebe, a large planetesimal in the outer Solar System. Icarus *219*, 86–109. https://doi.org/10.1016/J.ICARUS.2012.02.002.

74. Carter, P.J., and Stewart, S.T. (2020). Colliding in the Shadows of Giants: Planetesimal Collisions during the Growth and Migration of Gas Giants. Planet. Sci. J. *1*, 45. https://doi.org/10.3847/PSJ/abaecc.

75. Johnson, T.V., Mousis, O., Lunine, J.I., and Madhusudhan, N. (2012). Planetesimal compositions in exoplanet systems. Astrophys. J. *757*, 192. https://doi.org/10.1088/0004-637X/757/2/192.

76. Yokoyama, K., Kimura, Y., and Kaito, C. (2017). Experiments on Condensation of Calcium Sulfide Grains to Demarcate Environments for the Formation of Enstatite Chondrites. ACS Earth Space Chem. *1*, 601–607. https://doi.org/10.1021/ACSEARTHSPACECHEM.7B00076.

77. Greenwood, R.C., Franchi, I.A., Jambon, A., and Buchanan, P.C. (2005). Widespread magma oceans on asteroidal bodies in the early Solar System. Nature *435*, 916–918. https://doi.org/10.1038/nature03612.

78. MAYNE, R.G., SUNSHINE, J.M., McSWEEN, H.Y., McCOY, T.J., CORRIGAN, C.M., and GALE, A. (2010). Petrologic insights from the spectra of the unbrecciated eucrites: Implications for Vesta and basaltic asteroids. Meteorit. Planet. Sci. *45*, 1074–1092. https://doi.org/10.1111/J.1945-5100.2010.01090.X.

79. Mayne, R.G., Sunshine, J.M., McSween, H.Y., Bus, S.J., and McCoy, T.J. (2011). The origin of Vesta's crust: Insights from spectroscopy of the Vestoids. Icarus *214*, 147–160. https://doi.org/10.1016/J.ICARUS.2011.04.013.

80. Wilson, L., Goodrich, C.A., and Van Orman, J.A. (2008). Thermal evolution and physics of melt extraction on the ureilite parent body. Geochim. Cosmochim. Acta *72*, 6154–6176. https://doi.org/10.1016/j.gca.2008.09.025.

81. Monnereau, M., Guignard, J., Néri, A., Toplis, M.J., and Quitté, G. (2023). Differentiation time scales of small rocky bodies. Icarus *390*, 115294. https://doi.org/10.1016/J.ICARUS.2022.115294.

82. Collinet, M., and Grove, T.L. (2020). Widespread production of silica- and alkali-rich melts at the onset of planetesimal melting. Geochim. Cosmochim. Acta *277*, 334–357. https://doi.org/10.1016/J.GCA.2020.03.005.

83. Zhang, Z., Bercovici, D., and Elkins-Tanton, L.T. (2023). Melt migration in rubble-pile planetesimals: Implications for the formation of primitive achondrites. Earth Planet. Sci. Lett. *605*, 118019. https://doi.org/10.1016/J.EPSL.2023.118019.

84. Sunshine, J.M., Connolly, H.C., McCoy, T.J., Bus, S.J., and La Croix, L.M. (2008). Ancient asteroids enriched in refractory inclusions. Science *320*, 514–517. https://doi.org/10.1126/SCIENCE.1154340.

85. Cameron, A.G.W., and Truran, J.W. (1977). The supernova trigger for formation of the solar system. Icarus *30*, 447–461. https://doi.org/10.1016/0019-1035(77)90101-4.

86. Foster, P.N., Boss, A.P., Foster, P.N., and Boss, A.P. (1996). Triggering Star Formation with Stellar Ejecta. ApJ *468*, 784. https://doi.org/10.1086/177735.

87. Sahijpal, S., and Goswami, J.N. (1998). Refractory Phases in Primitive Meteorites Devoid of 26Al and 41Ca:Representative Samples of First Solar System Solids? Astrophys. J. *509*, L137–L140. https://doi.org/10.1086/311778.

88. Sunshine, J.M., Bus, S.J., Corrigan, C.M., McCoy, T.J., and Burbine, T.H. (2007). Olivine-dominated asteroids and meteorites: Distinguishing nebular and igneous histories. Meteorit. Planet. Sci. *42*, 155–170. https://doi.org/10.1111/J.1945-5100.2007.TB00224.X.

89. Tholen, D. (1984). Asteroid Taxonomy from Cluster Analysis of Photometry. PhD Thesis.

90. Suttle, M.D., Folco, L., Genge, M.J., Russell, S.S., Najorka, J., and van Ginneken, M. (2019). Intense aqueous alteration on C-type asteroids: Perspectives from giant fine-grained micrometeorites. Geochim. Cosmochim. Acta *245*, 352–373. https://doi.org/10.1016/J.GCA.2018.11.019.

91. Norton, O.R. (2002). The Cambridge Encyclopedia of Meteorites (Cambridge University Press).

92. Harju, E.R., Rubin, A.E., Ahn, I., Choi, B.G., Ziegler, K., and Wasson, J.T. (2014). Progressive aqueous alteration of CR carbonaceous chondrites. Geochim. Cosmochim. Acta *139*, 267–292. https://doi.org/10.1016/J.GCA.2014.04.048.

93. Müller, T.G., Ďurech, J., Ishiguro, M., Mueller, M., Krühler, T., Yang, H., Kim, M.J., O'Rourke, L., Usui, F., Kiss, C., et al. (2017). Hayabusa-2 mission target asteroid 162173 Ryugu (1999 JU3): Searching for the object's spin-axis orientation. Astron. Astrophys. *599*, A103. https://doi.org/10.1051/0004-6361/201629134.

94. Hamilton, V.E., Simon, A.A., Christensen, P.R., Reuter, D.C., Clark, B.E., Barucci, M.A., Bowles, N.E., Boynton, W.V., Brucato, J.R., Cloutis, E.A., et al. (2019). Evidence for widespread hydrated minerals on asteroid (101955) Bennu. Nat. Astron. *3*, 332–340. https://doi.org/10.1038/s41550-019-0722-2.

95. Tomeoka, K., and Buseck, P.R. (1985). Indicators of aqueous alteration in CM carbonaceous chondrites: Microtextures of a layered mineral containing Fe, S, O and Ni. Geochim. Cosmochim. Acta *49*, 2149–2163. https://doi.org/10.1016/0016-7037(85)90073-0.

96. Browning, L.B., McSween, H.Y., and Zolensky, M.E. (1996). Correlated alteration effects in CM carbonaceous chondrites. Geochim. Cosmochim. Acta *60*, 2621–2633. https://doi.org/10.1016/0016-7037(96)00121-4.

97. Hanowski, N.P., and Brearley, A.J. (2001). Aqueous alteration of chondrules in the CM carbonaceous chondrite, Allan Hills 81002: implications for parent body alteration. Geochim. Cosmochim. Acta *65*, 495–518. https://doi.org/10.1016/S0016-7037(00)00552-4.

98. Velbel, M.A., Tonui, E.K., and Zolensky, M.E. (2012). Replacement of olivine by serpentine in the carbonaceous chondrite Nogoya (CM2). Geochim. Cosmochim. Acta *87*, 117–135. https://doi.org/10.1016/J.GCA.2012.03.016.

99. Pignatelli, I., Marrocchi, Y., Vacher, L.G., Delon, R., and Gounelle, M. (2016). Multiple precursors of secondary mineralogical assemblages in CM chondrites. Meteorit. Planet. Sci. *51*, 785–805. https://doi.org/10.1111/MAPS.12625.

100. McSween, H.Y. (1977). On the nature and origin of isolated olivine grains in carbonaceous chondrites. Geochim. Cosmochim. Acta *41*, 411–418. https://doi.org/10.1016/0016-7037(77)90269-1.

101. Richardson, S.M., and McSween, H.Y. (1978). Textural evidence bearing on the origin of isolated olivine crystals in C2 carbonaceous chondrites. Earth Planet. Sci. Lett. *37*, 485–491. https://doi.org/10.1016/0012-821X(78)90064-X.

102. Jones, R.H. (1992). On the relationship between isolated and chondrule olivine grains in the carbonaceous chondrite ALHA77307. Geochim. Cosmochim. Acta *56*, 467–482. https://doi.org/10.1016/0016-7037(92)90145-9.

103. Olsen, E., and Grossman, L. (1978). On the origin of isolated olivine grains in type 2 carbonaceous chondrites. Earth Planet. Sci. Lett. *41*, 111–127. https://doi.org/10.1016/0012-821X(78)90001-8.

104. Krot, A.N., Petaev, M.I., Russell, S.S., Itoh, S., Fagan, T.J., Yurimoto, H., Chizmadia, L., Weisberg, M.K., Komatsu, M., Ulyanov, A.A., et al. (2004). Amoeboid olivine aggregates and related objects in carbonaceous chondrites: records of nebular and asteroid processes. Geochemistry *64*, 185–239. https://doi.org/10.1016/J.CHEMER.2004.05.001.

105. Sheng, Y.J., Hutcheon, I.D., and Wasserburg, G.J. (1991). Origin of plagioclase-olivine inclusions in carbonaceous chondrites. Geochim. Cosmochim. Acta *55*, 581–599. https://doi.org/10.1016/0016-7037(91)90014-V.

106. Jacquet, E., Piralla, M., Kersaho, P., and Marrocchi, Y. (2021). Origin of isolated olivine grains in carbonaceous chondrites. Meteorit. Planet. Sci. *56*, 13–33. https://doi.org/10.1111/MAPS.13583.

107. Desnoyers, C. (1980). The Niger (I) carbonaceous chondrite and implications for the origin of aggregates and isolated olivine grains in C2 chondrites. Earth Planet. Sci. Lett. *47*, 223–234. https://doi.org/10.1016/0012-821X(80)90038-2.

108. Johnson, B.C., Minton, D.A., Melosh, H.J., and Zuber, M.T. (2015). Impact jetting as the origin of chondrules. Nature *517*, 339–341. https://doi.org/10.1038/nature14105.

109. Ringwood, A.E. (1963). The origin of high-temperature minerals in carbonaceous chondrites. J. Geophys. Res. *68*, 1141–1143. https://doi.org/10.1029/JZ068I004P01141.

110. Anders, E. (1975). Do stony meteorites come from comets? Icarus *24*, 363–371. https://doi.org/10.1016/0019-1035(75)90132-3.

111. McSween, H.Y. (1979). Are carbonaceous chondrites primitive or processed? A review. Rev. Geophys. *17*, 1059–1078. https://doi.org/10.1029/RG017I005P01059.

112. Sugimoto, C., Tatsumi, E., Cho, Y., Morota, T., Honda, R., Kameda, S., Yokota, Y., Yumoto, K., Aoki, M., DellaGiustina, D.N., et al. (2021). High-resolution observations of bright boulders on asteroid Ryugu: 2. Spectral properties. Icarus *369*, 114591. https://doi.org/10.1016/J.ICARUS.2021.114591.

113. Clark, B.E., Binzel, R.P., Howell, E.S., Cloutis, E.A., Ockert-Bell, M., Christensen, P., Barucci, M.A., DeMeo, F., Lauretta, D.S., Connolly, H., et al. (2011). Asteroid (101955) 1999 RQ36: Spectroscopy from 0.4 to 2.4 μm and meteorite analogs. Icarus *216*, 462–475. https://doi.org/10.1016/J.ICARUS.2011.08.021.

114. Hergenrother, C.W., Nolan, M.C., Binzel, R.P., Cloutis, E.A., Barucci, M.A., Michel, P., Scheeres, D.J., d'Aubigny, C.D., Lazzaro, D., Pinilla-Alonso, N., et al. (2013). Lightcurve, Color and Phase Function Photometry of the OSIRIS-REx Target Asteroid (101955) Bennu. Icarus *226*, 663–670. https://doi.org/10.1016/J.ICARUS.2013.05.044.

115. Lauretta, D.S., Balram-Knutson, S.S., Beshore, E., Boynton, W.V., Drouet d'Aubigny, C., DellaGiustina, D.N., Enos, H.L., Golish, D.R., Hergenrother, C.W., Howell, E.S., et al. (2017). OSIRIS-REx: Sample Return from Asteroid (101955) Bennu. Space Sci. Rev. *212*, 925–984. https://doi.org/10.1007/S11214-017-0405-1.

116. Barnouin, O.S., Daly, M.G., Palmer, E.E., Gaskell, R.W., Weirich, J.R., Johnson, C.L., Asad, M.M.A., Roberts, J.H., Perry, M.E., Susorney, H.C.M., et al. (2019). Shape of (101955) Bennu indicative of a rubble pile with internal stiffness. Nat. Geosci. *12*, 247–252. https://doi.org/10.1038/s41561-019-0330-x.

117. Walsh, K.J., Jawin, E.R., Ballouz, R.L., Barnouin, O.S., Bierhaus, E.B., Connolly, H.C., Molaro, J.L., McCoy, T.J., Delbo', M., Hartzell, C.M., et al. (2019). Craters, boulders and regolith of (101955) Bennu indicative of an old and dynamic surface. Nat. Geosci. *12*, 242–246. https://doi.org/10.1038/s41561-019-0326-6.

118. Emery, J.P., Fernández, Y., Kelley, M.S.P., Warden nèe Crane, K., Hergenrother, C., Lauretta, D.S., Drake, M.J., Campins, H., and Ziffer, J. (2014). Thermal infrared observations and thermophysical characterization of OSIRIS-REx target asteroid (101955) Bennu. Icarus *234*, 17–35. https://doi.org/10.1016/J.ICARUS.2014.02.005.

119. Scheeres, D.J., McMahon, J.W., French, A.S., Brack, D.N., Chesley, S.R., Farnocchia, D., Takahashi, Y., Leonard, J.M., Geeraert, J., Page, B., et al. (2019). The dynamic geophysical environment of (101955) Bennu based on OSIRIS-REx measurements. Nat. Astron. *3*, 352–361. https://doi.org/10.1038/s41550-019-0721-3.

120. Lauretta, D.S., Bartels, A.E., Barucci, M.A., Bierhaus, E.B., Binzel, R.P., Bottke, W.F., Campins, H., Chesley, S.R., Clark, B.C., Clark, B.E., et al. (2015). The OSIRIS-REx target asteroid (101955) Bennu: Constraints on its physical, geological, and dynamical nature from astronomical observations. Meteorit. Planet. Sci. *50*, 834–849. https://doi.org/10.1111/MAPS.12353.

121. Campins, H., Morbidelli, A., Tsiganis, K., de León, J., Licandro, J., and Lauretta, D. (2010). THE ORIGIN OF ASTEROID 101955 (1999 RQ36). Astrophys. J. *721*, L53–L57. https://doi.org/10.1088/2041-8205/721/1/L53.

122. Walsh, K.J., Delbó, M., Bottke, W.F., Vokrouhlický, D., and Lauretta, D.S. (2013). Introducing the Eulalia and new Polana asteroid families: Re-assessing primitive asteroid families in the inner Main Belt. Icarus *225*, 283–297. https://doi.org/10.1016/J.ICARUS.2013.03.005.

123. Bottke, W.F., Vokrouhlický, D., Walsh, K.J., Delbo, M., Michel, P., Lauretta, D.S., Campins, H., Connolly, H.C., Scheeres, D.J., and Chelsey, S.R. (2015). In search of the source of asteroid (101955) Bennu: Applications of the stochastic YORP model. Icarus *247*, 191–217. https://doi.org/10.1016/J.ICARUS.2014.09.046.

124. Campins, H., Hargrove, K., Pinilla-Alonso, N., Howell, E.S., Kelley, M.S., Licandro, J., Mothé-Diniz, T., Fernández, Y., and Ziffer, J. (2010). Water ice and organics on the surface of the asteroid 24 Themis. Nature *464*, 1320–1321. https://doi.org/10.1038/nature09029.

125. Rivkin, A.S., and Emery, J.P. (2010). Detection of ice and organics on an asteroidal surface. Nature *464*, 1322–1323. https://doi.org/10.1038/nature09028.

126. Hsieh, H.H., Jewitt, D.C., and Fernández, Y.R. (2004). The Strange Case of 133P/Elst-Pizarro: A Comet among the Asteroids. Astron. J. *127*, 2997–3017. https://doi.org/10.1086/383208.

127. Breitenfeld, L.B., Rogers, A.D., Glotch, T.D., Hamilton, V.E., Christensen, P.R., Lauretta, D.S., Gemma, M.E., Howard, K.T., Ebel, D.S., Kim, G., et al. (2021). Machine Learning Mid-Infrared Spectral Models for Predicting Modal Mineralogy of CI/CM Chondritic Asteroids and Bennu. JGR. Planets *126*. e2021JE007035. https://doi.org/10.1029/2021JE007035.

128. Huss, G., Rubin, A., and Grossman, J. (2006). Thermal Metamorphism in Cjondrites. In Meteorites and the Early Solar System II, pp. 567–586.

129. Wood, J.A. (1962). Metamorphism in chondrites. Geochim. Cosmochim. Acta *26*, 739–749. https://doi.org/10.1016/0016-7037(62)90036-4.

130. Tomkins, A.G., Johnson, T.E., and Mitchell, J.T. (2020). A review of the chondrite–achondrite transition, and a metamorphic facies series for equilibrated primitive stony meteorites. Meteorit. Planet. Sci. *55*, 857–885. https://doi.org/10.1111/MAPS.13472.

131. Sugita, S., Honda, R., Morota, T., Kameda, S., Sawada, H., Tatsumi, E., Yamada, M., Honda, C., Yokota, Y., Kouyama, T., et al. (2019). The geomorphology, color, and thermal properties of Ryugu: Implications for parent-body processes. Science *364*, 252. https://doi.org/10.1126/SCIENCE.AAW0422.

132. Watanabe, S., Hirabayashi, M., Hirata, N., Hirata, N., Noguchi, R., Shimaki, Y., Ikeda, H., Tatsumi, E., Yoshikawa, M., Kikuchi, S., et al. (2019). Hayabusa2 arrives at the carbonaceous asteroid 162173 Ryugu-A spinning top-shaped rubble pile. Science *364*, 268–272. https://doi.org/10.1126/SCIENCE.AAV8032.

133. Grott, M., Biele, J., Michel, P., Sugita, S., Schröder, S., Sakatani, N., Neumann, W., Kameda, S., Michikami, T., and Honda, C. (2020). Macroporosity and Grain Density of Rubble Pile Asteroid (162173). J. Geophys. Res. Planets *125*. e2020JE006519. https://doi.org/10.1029/2020JE006519.

134. Tatsumi, E., Sakatani, N., Riu, L., Matsuoka, M., Honda, R., Morota, T., Kameda, S., Nakamura, T., Zolensky, M., Brunetto, R., et al. (2021). Spectrally blue hydrated parent body of asteroid (162173) Ryugu. Nat. Commun. *12*, 5837. https://doi.org/10.1038/s41467-021-26071-8.

135. Yada, T., Abe, M., Okada, T., Nakato, A., Yogata, K., Miyazaki, A., Hatakeda, K., Kumagai, K., Nishimura, M., Hitomi, Y., et al. (2021). Preliminary analysis of the Hayabusa2 samples returned from C-type asteroid Ryugu. Nat. Astron. *6*, 214–220. https://doi.org/10.1038/s41550-021-01550-6.

136. Zolensky, M.E., Nakamura, K., Gounelle, M., Mikouchi, T., Kasama, T., Tachikawa, O., and Tonui, E. (2002). Mineralogy of Tagish Lake: An ungrouped type 2 carbonaceous chondrite. Meteorit. Planet. Sci. *37*, 737–761. https://doi.org/10.1111/J.1945-5100.2002.TB00852.X.

137. Neumann, W., Grott, M., Trieloff, M., Jaumann, R., Biele, J., Hamm, M., and Kührt, E. (2021). Microporosity and parent body of the rubble-pile NEA (162173) Ryugu. Icarus *358*, 114166. https://doi.org/10.1016/J.ICARUS.2020.114166.

138. Flynn, G.J., Consolmagno, G.J., Brown, P., and Macke, R.J. (2018). Physical properties of the stone meteorites: Implications for the properties of their parent bodies. Geochemistry *78*, 269–298. https://doi.org/10.1016/J.CHEMER.2017.04.002.

139. Nakamura, E., Kobayashi, K., Tanaka, R., Kunihiro, T., Kitagawa, H., Potiszil, C., Ota, T., Sakaguchi, C., Yamanaka, M., Ratnayake, D.M., et al. (2022). On the origin and evolution of the asteroid Ryugu: A comprehensive geochemical perspective. Proc. Jpn. Acad. Ser. B *98*, 227–282. https://doi.org/10.2183/PJAB.98.015.

140. Drolshagen, G., Koschny, D., Drolshagen, S., Kretschmer, J., and Poppe, B. (2017). Mass accumulation of earth from interplanetary dust, meteoroids, asteroids and comets. Planet. Space Sci. *143*, 21–27. https://doi.org/10.1016/J.PSS.2016.12.010.

141. Cloutis, E.A., Hudon, P., Hiroi, T., Gaffey, M.J., and Mann, P. (2012). Spectral reflectance properties of carbonaceous chondrites: 8. "Other" carbonaceous chondrites: CH, ungrouped, polymict, xenolithic inclusions, and R chondrites. Icarus *221*, 984–1001. https://doi.org/10.1016/J.ICARUS.2012.10.008.

142. Jaumann, R., Schmitz, N., Ho, T.M., Schröder, S.E., Otto, K.A., Stephan, K., Elgner, S., Krohn, K., Preusker, F., Scholten, F., et al. (2019). Images from the surface of asteroid Ryugu show rocks similar to carbonaceous chondrite meteorites. Science *365*, 817–820. https://doi.org/10.1126/SCIENCE.AAW8627.

143. Sakatani, N., Tanaka, S., Okada, T., Fukuhara, T., Riu, L., Sugita, S., Honda, R., Morota, T., Kameda, S., Yokota, Y., et al. (2021). Anomalously porous boulders on (162173) Ryugu as primordial materials from its parent body. Nat. Astron. *5*, 766–774. https://doi.org/10.1038/s41550-021-01371-7.

144. Weiss, B.P., and Elkins-Tanton, L.T. (2013). Differentiated Planetesimals and the Parent Bodies of Chondrites. Annu. Rev. Earth Planet. Sci. *41*, 529–560. https://doi.org/10.1146/ANNUREV-EARTH-040610-133520.

145. Nakamura, T., Matsumoto, M., Amano, K., Enokido, Y., Zolensky, M.E., Mikouchi, T., Genda, H., Tanaka, S., Zolotov, M.Y., Kurosawa, K., et al. (2023). Formation and evolution of carbonaceous asteroid Ryugu: Direct evidence from returned samples. Science *379*, eabn8671. https://doi.org/10.1126/SCIENCE.ABN8671.

146. Nakashima, D., Nakamura, T., Zhang, M., Kita, N.T., Mikouchi, T., Yoshida, H., Enokido, Y., Morita, T., Kikuiri, M., Amano, K., et al. (2023). Chondrule-like objects and Ca-Al-rich inclusions in Ryugu may potentially be the oldest Solar System materials. Nat. Commun. *14*, 532. https://doi.org/10.1038/s41467-023-36268-8.

147. Russell, C.T., Raymond, C.A., Coradini, A., McSween, H.Y., Zuber, M.T., Nathues, A., De Sanctis, M.C., Jaumann, R., Konopliv, A.S., Preusker, F., et al. (2012). Dawn at vesta: Testing the protoplanetary paradigm. Science *336*, 684–686. https://doi.org/10.1126/SCIENCE.1219381.

148. McCoy, T.J., Beck, A.W., Prettyman, T.H., and Mittlefehldt, D.W. (2015). Asteroid (4) Vesta II: Exploring a geologically and geochemically complex world with the Dawn Mission. Geochemistry *75*, 273–285. https://doi.org/10.1016/j.chemer.2014.12.001.

149. Moskovitz, N.A., Willman, M., Burbine, T.H., Binzel, R.P., and Bus, S.J. (2010). A spectroscopic comparison of HED meteorites and V-type asteroids in the inner Main Belt. Icarus *208*, 773–788. https://doi.org/10.1016/J.ICARUS.2010.03.002.

150. Ieva, S., Dotto, E., Lazzaro, D., Perna, D., Fulvio, D., and Fulchignoni, M. (2016). Spectral characterization of V-type asteroids – II. A statistical analysis. Mon. Not. R. Astron. Soc. *455*, 2871–2888. https://doi.org/10.1093/MNRAS/STV2510.

151. Palomba, E., Longobardo, A., De Sanctis, M.C., Zinzi, A., Ammannito, E., Marchi, S., Tosi, F., Zambon, F., Capria, M.T., Russell, C.T., et al. (2015). Detection of new olivine-rich locations on Vesta. Icarus *258*, 120–134. https://doi.org/10.1016/J.ICARUS.2015.06.011.

152. Ammannito, E., De Sanctis, M.C., Palomba, E., Longobardo, A., Mittlefehldt, D.W., McSween, H.Y., Marchi, S., Capria, M.T., Capaccioni, F., Frigeri, A., et al. (2013).

Olivine in an unexpected location on Vesta's surface. Nature *504*, 122–125. https://doi.org/10.1038/nature12665.

153. Barrat, J.A., Yamaguchi, A., Zanda, B., Bollinger, C., and Bohn, M. (2010). Relative chronology of crust formation on asteroid Vesta: Insights from the geochemistry of diogenites. Geochim. Cosmochim. Acta *74*, 6218–6231. https://doi.org/10.1016/J.GCA.2010.07.028.

154. Righter, K., and Drake, M.J. (1997). A magma ocean on Vesta: Core formation and petrogenesis of eucrites and diogenites. Meteorit. Planet. Sci. *32*, 929–944. https://doi.org/10.1111/J.1945-5100.1997.TB01582.X.

155. Yamaguchi, A., Barrat, J.A., Greenwood, R.C., Shirai, N., Okamoto, C., Setoyanagi, T., Ebihara, M., Franchi, I.A., and Bohn, M. (2009). Crustal partial melting on Vesta: Evidence from highly metamorphosed eucrites. Geochim. Cosmochim. Acta *73*, 7162–7182. https://doi.org/10.1016/j.gca.2009.07.037.

156. Shearer, C.K., Burger, P., and Papike, J.J. (2010). Petrogenetic relationships between diogenites and olivine diogenites: Implications for magmatism on the HED parent body. Geochim. Cosmochim. Acta *74*, 4865–4880. https://doi.org/10.1016/J.GCA.2010.05.015.

157. Ghosh, A., and McSween, H.Y. (1998). A Thermal Model for the Differentiation of Asteroid 4 Vesta, Based on Radiogenic Heating. Icarus *134*, 187–206. https://doi.org/10.1006/icar.1998.5956.

158. Neumann, W., Breuer, D., and Spohn, T. (2014). Differentiation of Vesta: Implications for a shallow magma ocean. Earth Planet. Sci. Lett. *395*, 267–280. https://doi.org/10.1016/J.EPSL.2014.03.033.

159. Hewins, R.H., and Ulmer, G.C. (1984). Intrinsic oxygen fugacities of diogenites and mesosiderite clasts. Geochim. Cosmochim. Acta *48*, 1555–1560. https://doi.org/10.1016/0016-7037(84)90410-1.

160. McSween, H.Y., Mittlefehldt, D.W., Beck, A.W., Mayne, R.G., and McCoy, T.J. (2010). HED Meteorites and Their Relationship to the Geology of Vesta and the Dawn Mission. In The Dawn Mission to Minor Planets 4 Vesta and 1 Ceres (Springer), pp. 141–174. https://doi.org/10.1007/978-1-4614-4903-4_9.

161. O'D Alexander, C.M., Boss, A.P., and Carlson, R.W. (2001). The Early Evolution of the Inner Solar System: A Meteoritic Perspective. Science *293*, 64–68. https://doi.org/10.1126/SCIENCE.1052872.

162. Qin, L., He, X.W., Li, W.Y., Zhang, Y.K., and Janney, P.E. (2008). Rapid accretion and differentiation of iron meteorite parent bodies inferred from 182Hf–182W chronometry and thermal modeling. J. Chromatogr. A *1187*, 94–102. https://doi.org/10.1016/J.EPSL.2008.06.018.

163. Lugmair, G.W., and Shukolyukov, A. (1998). Early solar system timescales according to 53Mn-53Cr systematics. Geochim. Cosmochim. Acta *62*, 2863–2886. https://doi.org/10.1016/S0016-7037(98)00189-6.

164. Woolum, D.S., and Cassen, P. (1999). Astronomical constraints on nebular temperatures: Implications for planetesimal formation. Meteorit. Planet. Sci. *34*, 897–907. https://doi.org/10.1111/J.1945-5100.1999.TB01408.X.

165. McCubbin, F.M., Lewis, J.A., Barnes, J.J., Elardo, S.M., and Boyce, J.W. (2021). The abundances of F, Cl, and H2O in eucrites: Implications for the origin of volatile depletion in the asteroid 4 Vesta. Geochim. Cosmochim. Acta *314*, 270–293. https://doi.org/10.1016/J.GCA.2021.08.021.

166. Lucas, M.P., Emery, J.P., Hiroi, T., and McSween, H.Y. (2019). Spectral properties and mineral compositions of acapulcoite–lodranite clan meteorites: Establishing S-type asteroid–meteorite connections. Meteorit. Planet. Sci. *54*, 157–180. https://doi.org/10.1111/MAPS.13203.

167. Sunshine, J.M., Bus, S.J., McCoy, T.J., Burbine, T.H., Corrigan, C.M., and Binzel, R.P. (2004). High-calcium pyroxene as an indicator of igneous differentiation in asteroids and meteorites. Meteorit. Planet. Sci. *39*, 1343–1357. https://doi.org/10.1111/J.1945-5100.2004.TB00950.X.

168. Carruba, V., Huaman, M.E., Domingos, R.C., Santos, C.R.D., and Souami, D. (2014). Dynamical evolution of V-type asteroids in the central main belt. Mon. Not. R. Astron. Soc. *439*, 3168–3179. https://doi.org/10.1093/MNRAS/STU192.

169. Gaffey, M.J., Bell, J.F., Brown, R., Burbine, T.H., Piatek, J.L., Reed, K.L., and Chaky, D.A. (1993). Mineralogical Variations within the S-Type Asteroid Class. Icarus *106*, 573–602. https://doi.org/10.1006/icar.1993.1194.

170. Noonan, J.W., Reddy, V., Harris, W.M., Bottke, W.F., Sanchez, J.A., Furfaro, R., Brown, Z., Fernandes, R., Kareta, T., Lejoly, C., et al. (2019). Search for the H Chondrite Parent Body among the Three Largest S-type Asteroids: (3) Juno, (7) Iris, and (25) Phocaea. Astron. J. *158*, 213. https://doi.org/10.3847/1538-3881/AB4813.

171. Ghosh, A., Weidenschilling, S.J., and McSween, H.Y. (2003). Importance of the accretion process in asteroid thermal evolution: 6 Hebe as an example. Meteorit. Planet. Sci. *38*, 711–724. https://doi.org/10.1111/J.1945-5100.2003.TB00036.X.

172. Gaffey, M.J., and Gilbert, S.L. (1998). Asteroid 6 Hebe: The probable parent body of the H-type ordinary chondrites and the IIE iron meteorites. Meteorit. Planet. Sci. *33*, 1281–1295. https://doi.org/10.1111/J.1945-5100.1998.TB01312.X.

173. Monnereau, M., Toplis, M.J., Baratoux, D., and Guignard, J. (2013). Thermal history of the H-chondrite parent body: Implications for metamorphic grade and accretionary time-scales. Geochim. Cosmochim. Acta *119*, 302–321. https://doi.org/10.1016/J.GCA.2013.05.035.

174. Henke, S., Gail, H.P., Trieloff, M., and Schwarz, W.H. (2013). Thermal evolution model for the H chondrite asteroid-instantaneous formation versus protracted accretion. Icarus *226*, 212–228. https://doi.org/10.1016/J.ICARUS.2013.05.034.

175. Sahijpal, S. (2021). Thermal evolution of non-spherical asteroids in the early solar system. Icarus *362*, 114439. https://doi.org/10.1016/J.ICARUS.2021.114439.

176. Scott, E.R., and Wilson, L. (2005). Meteoritic and other constraints on the internal structure and impact history of small asteroids. Icarus *174*, 46–53. https://doi.org/10.1016/J.ICARUS.2004.10.014.

177. Abe, S., Mukai, T., Hirata, N., Barnouin-Jha, O.S., Cheng, A.F., Demura, H., Gaskell, R.W., Hashimoto, T., Hiraoka, K., Honda, T., et al. (2006). Mass and local topography measurements of Itokawa by Hayabusa. Science *312*, 1344–1347. https://doi.org/10.1126/SCIENCE.1126272.

178. Yano, H., Kubota, T., Miyamoto, H., Okada, T., Scheeres, D., Takagi, Y., Yoshida, K., Abe, M., Abe, S., Barnouin-Jha, O., et al. (2006). Touchdown of the Hayabusa spacecraft at the muses sea on Itokawa. Science *312*, 1350–1353. https://doi.org/10.1126/SCIENCE.1126164.

179. Fujiwara, A., Kawaguchi, J., Yeomans, D.K., Abe, M., Mukai, T., Okada, T., Saito, J., Yano, H., Yoshikawa, M., Scheeres, D.J., et al. (2006). The rubble-pile asteroid Itokawe as observed by Hayabusa. Science *312*, 1330–1334. https://doi.org/10.1126/SCIENCE.1125841.

180. Miyamoto, H., Yano, H., Scheeres, D.J., Abe, S., Barnouin-Jha, O., Cheng, A.F., Demura, H., Gaskell, R.W., Hirata, N., Ishiguro, M., et al. (2007). Regolith migration and sorting on asteroid Itokawa. Science *316*, 1011–1014. https://doi.org/10.1126/SCIENCE.1134390.

181. Hirata, N., Barnouin-Jha, O.S., Honda, C., Nakamura, R., Miyamoto, H., Sasaki, S., Demura, H., Nakamura, A.M., Michikami, T., Gaskell, R.W., et al. (2009). A survey of possible impact structures on 25143 Itokawa. Icarus *200*, 486–502. https://doi.org/10.1016/J.ICARUS.2008.10.027.

182. Okada, T., Shirai, K., Yamamoto, Y., Arai, T., Ogawa, K., Hosono, K., and Kato, M. (2006). X-ray flourescence spectrometry of asteroid Itokawa by Hayabusa. Science *312*, 1338–1341. https://doi.org/10.1126/SCIENCE.1125731.

183. Nagao, K., Okazaki, R., Nakamura, T., Miura, Y.N., Osawa, T., Bajo, K.I., Matsuda, S., Ebihara, M., Ireland, T.R., Kitajima, F., et al. (2011). Irradiation history of itokawa regolith material deduced from noble gases in the hayabusa samples. Science *333*, 1128–1131. https://doi.org/10.1126/SCIENCE.1207785.

184. Nakamura, T., Noguchi, T., Tanaka, M., Zolensky, M.E., Kimura, M., Tsuchiyama, A., Nakato, A., Ogami, T., Ishida, H., Uesugi, M., et al. (2011). Itokawa dust particles: A direct link between S-type asteroids and ordinary

chondrites. Science *333*, 1113–1116. https://doi.org/10.1126/SCIENCE.1207758.

185. Landsman, Z.A., Campins, H., Pinilla-Alonso, N., Hanuš, J., and Lorenzi, V. (2015). A new investigation of hydration in the M-type asteroids. Icarus *252*, 186–198. https://doi.org/10.1016/J.ICARUS.2015.01.021.

186. Tholen, D.J., and Barucci, M.A. (1989). Asteroid taxonomy. In Asteroids II (University of Arizona Press), pp. 298–315.

187. Ockert-Bell, M.E., Clark, B.E., Shepard, M.K., Rivkin, A.S., Binzel, R.P., Thomas, C.A., DeMeo, F.E., Bus, S.J., and Shah, S. (2008). Observations of X/M asteroids across multiple wavelengths. Icarus *195*, 206–219. https://doi.org/10.1016/J.ICARUS.2007.11.006.

188. Fornasier, S., Clark, B.E., Dotto, E., Migliorini, A., Ockert-Bell, M., and Barucci, M.A. (2010). Spectroscopic survey of M-type asteroids. Icarus *210*, 655–673. https://doi.org/10.1016/J.ICARUS.2010.07.001.

189. Carry, B. (2012). Density of asteroids. Planet. Space Sci. *73*, 98–118. https://doi.org/10.1016/J.PSS.2012.03.009.

190. Elkins-Tanton, L.T., Asphaug, E., Bell, J.F., Bercovici, H., Bills, B., Binzel, R., Bottke, W.F., Dibb, S., Lawrence, D.J., Marchi, S., et al. (2020). Observations, Meteorites, and Models: A Preflight Assessment of the Composition and Formation of (16) Psyche. J. Geophys. Res. Planets *125*. e2019JE006296. https://doi.org/10.1029/2019JE006296.

191. Marchis, F., Jorda, L., Vernazza, P., Brož, M., Hanuš, J., Ferrais, M., Vachier, F., Rambaux, N., Marsset, M., Viikinkoski, M., et al. (2021). (216) Kleopatra, a low density critically rotating M-type asteroid. Astron. Astrophys. *653*, A57. https://doi.org/10.1051/0004-6361/202140874.

192. Zhang, Z., Bercovici, D., and Elkins-Tanton, L. (2022). Cold Compaction and Macro-Porosity Removal in Rubble-Pile Asteroids: 1. JGR. Planets *127*. e2022JE007342. https://doi.org/10.1029/2022JE007342.

193. Shepard, M.K., Clark, B.E., Nolan, M.C., Howell, E.S., Magri, C., Giorgini, J.D., Benner, L.A., Ostro, S.J., Harris, A.W., Warner, B., et al. (2008). A radar survey of M- and X-class asteroids. Icarus *195*, 184–205. https://doi.org/10.1016/J.ICARUS.2007.11.032.

194. Ockert-Bell, M.E., Clark, B.E., Shepard, M.K., Isaacs, R.A., Cloutis, E.A., Fornasier, S., and Bus, S.J. (2010). The composition of M-type asteroids: Synthesis of spectroscopic and radar observations. Icarus *210*, 674–692. https://doi.org/10.1016/J.ICARUS.2010.08.002.

195. Cloutis, E.A., Gaffey, M.J., Smith, D.G.W., and Lambert, R.S.J. (1990). Metal silicate mixtures: Spectral properties and applications to asteroid taxonomy. J. Geophys. Res. *95*, 8323–8338. https://doi.org/10.1029/JB095IB06P08323.

196. Gaffey, M.J., Burbine, T.H., and Binzel, R.P. (1993). Asteroid spectroscopy: Progress and perspectives. Meteoritics *28*, 161–187. https://doi.org/10.1111/J.1945-5100.1993.TB00755.X.

197. Vilas, F. (1994). A Cheaper, Faster, Better Way to Detect Water of Hydration on Solar System Bodies. Icarus *111*, 456–467. https://doi.org/10.1006/ICAR.1994.1156.

198. Hardersen, P., Gaffey, M., and Abell, P. (2005). Near-IR spectral evidence for the presence of iron-poor orthopyroxenes on the surfaces of six M-type asteroids. Icarus *175*, 141–158. https://doi.org/10.1016/J.ICARUS.2004.10.017.

199. Hardersen, P.S., Cloutis, E.A., Reddy, V., Mothé-Diniz, T., and Emery, J.P. (2011). The M-/X-asteroid menagerie: Results of an NIR spectral survey of 45 main-belt asteroids. Meteorit. Planet. Sci. *46*, 1910–1938. https://doi.org/10.1111/J.1945-5100.2011.01304.X.

200. Rivkin, A., Howell, E.S., Lebofsky, L.A., Clark, B.E., and Britt, D.T. (2000). The Nature of M-Class Asteroids from 3-μm Observations. Icarus *145*, 351–368. https://doi.org/10.1006/ICAR.2000.6354.

201. Goldstein, J.I., Scott, E.R.D., and Chabot, N.L. (2009). Iron meteorites: Crystallization, thermal history, parent bodies, and origin. Geochemistry *69*, 293–325. https://doi.org/10.1016/J.CHEMER.2009.01.002.

202. Scott, E.R.D., Haack, H., and Love, S.G. (2001). Formation of mesosiderites by fragmentation and reaccretion of a large differentiated asteroid. Meteorit. Planet. Sci. *36*, 869–881. https://doi.org/10.1111/J.1945-5100.2001.TB01927.X.

203. A'Hearn, M.F. (1988). Observations of Cometary Nuclei. Annu. Rev. Earth Planet. Sci. *16*, 273–293. https://doi.org/10.1146/ANNUREV.EA.16.050188.001421.

204. Van Boekel, R., Min, M., Leinert, C., Waters, L.B.F.M., Richichi, A., Chesneau, O., Dominik, C., Jaffe, W., Dutrey, A., Graser, U., et al. (2004). The building blocks of planets within the 'terrestrial' region of protoplanetary disks. Nature *432*, 479–482. https://doi.org/10.1038/nature03088.

205. Campins, H., and Ryan, E.V. (1989). The identification of crystalline olivine in cometary silicates. Astrophys. J. *341*, 1059. https://doi.org/10.1086/167563.

206. Kelley, M.S., Woodward, C.E., Harker, D.E., Wooden, D.H., Gehrz, R.D., Campins, H., Hanner, M.S., Lederer, S.M., Osip, D.J., Pittichova, J., et al. (2006). A Spitzer Study of Comets 2P/Encke, 67P/Churyumov-Gerasimenko, and C/2001 HT50 (LINEAR-NEAT). Astrophys. J. *651*, 1256–1271. https://doi.org/10.1086/507701.

207. Hanner, M.S., Lynch, D.K., Russell, R.W., Hackwell, J.A., Kellogg, R., and Blaney, D. (1996). Mid-infrared spectra of comets P/Borrelly, P/Faye, and P/Schaumasse. Icarus *124*, 344–351. https://doi.org/10.1006/icar.1996.0209.

208. Hanner, M.S., Hackwell, J.A., Russell, R.W., and Lynch, D.K. (1994). Silicate Emission Feature in the Spectrum of Comet Mueller 1993a. Icarus *112*, 490–495. https://doi.org/10.1006/ICAR.1994.1200.

209. Wooden, D.H., Harker, D.E., Woodward, C.E., Butner, H.M., Koike, C., Witteborn, F.C., and McMurtry, C.W. (1999). Silicate Mineralogy of the Dust in the Inner Coma of Comet C/1995 01 (Hale-Bopp) Pre- and Postperihelion. Astrophys. J. *517*, 1034–1058. https://doi.org/10.1086/307206.

210. Harker, D.E., Woodward, C.E., Wooden, D.H., Fisher, R.S., and Trujillo, C.A. (2007). Gemini-N mid-IR observations of the dust properties of the ejecta excavated from Comet 9P/Tempel 1 during Deep Impact. Icarus *191*, 432–453. https://doi.org/10.1016/J.ICARUS.2007.03.039.

211. Kelley, M.S., Woodward, C.E., Gehrz, R.D., Reach, W.T., and Harker, D.E. (2017). Mid-infrared spectra of comet nuclei. Icarus *284*, 344–358. https://doi.org/10.1016/J.ICARUS.2016.11.029.

212. Reach, W.T., Vaubaillon, J., Lisse, C.M., Holloway, M., and Rho, J. (2010). Explosion of Comet 17P/Holmes as revealed by the Spitzer Space Telescope. Icarus *208*, 276–292. https://doi.org/10.1016/J.ICARUS.2010.01.020.

213. Ootsubo, T., Kawakita, H., Shinnaka, Y., Watanabe, J.i., and Honda, M. (2020). Unidentified infrared emission features in mid-infrared spectrum of comet 21P/Giacobini-Zinner. Icarus *338*, 113450. https://doi.org/10.1016/J.ICARUS.2019.113450.

214. Sarmecanic, J., Fomenkova, M., Jones, B., and Lavezzi, T. (1997). Constraints on the Nucleus and Dust Properties from Mid-Infrared Imaging of Comet Hyakutake. Astrophys. J. *483*, L69–L72. https://doi.org/10.1086/310726.

215. Lynch, D.K., Russell, R.W., and Sitko, M.L. (2002). 3- to 14-μm Spectroscopy of Comet C/1999 T1 (McNaught–Hartley). Icarus *159*, 234–238. https://doi.org/10.1006/ICAR.2002.6882.

216. Schambeau, C.A., Fernández, Y.R., Lisse, C.M., Samarasinha, N., and Woodney, L.M. (2015). A new analysis of Spitzer observations of Comet 29P/Schwassmann-Wachmann 1. Icarus *260*, 60–72. https://doi.org/10.1016/j.icarus.2015.06.038.

217. Lynch, D., Russell, R.W., and Sitko, M.L. (2000). 3- to 14- μm Spectroscopy of Comet 55P/Tempel–Tuttle, Parent Body of the Leonid Meteors. Icarus *144*, 187–190. https://doi.org/10.1006/ICAR.1999.6260.

218. Sitko, M.L., Lynch, D.K., Russell, R.W., and Hanner, M.S. (2004). 3–14 Micron Spectroscopy of Comets C/2002 O4 (Honig), C/2002 V1 (NEAT), C/2002 X5 (Kudo-Fujikawa), C/2002 Y1 (Juels-Holvorcem), and 69P/Taylor and the Relationships among Grain Temperature, Silicate Band Strength, and

Structure among Comet Families. Astrophys. J. *612*, 576–587. https://doi.org/10.1086/421991.

219. Fulle, M., Della Corte, V., Rotundi, A., Rietmeijer, F.J.M., Green, S.F., Weissman, P., Accolla, M., Colangeli, L., Ferrari, M., Ivanovski, S., et al. (2016). Comet 67P/Churyumov–Gerasimenko preserved the pebbles that formed planetesimals. Mon. Not. R. Astron. Soc. *462*, S132–S137. https://doi.org/10.1093/MNRAS/STW2299.

220. Lisse, C., Bauer, J., Cruikshank, D., Emery, J., Fernández, Y., Fernández-Valenzuela, E., Kelley, M., McKay, A., Reach, W., Pendleton, Y., et al. (2020). Spitzer's Solar System studies of comets, centaurs and Kuiper belt objects. Nat. Astron. *4*, 930–939. https://doi.org/10.1038/s41550-020-01219-6.

221. Meech, K.J., A'Hearn, M.F., Adams, J.A., Bacci, P., Bai, J., Barrera, L., Battelino, M., Bauer, J.M., Becklin, E., Bhatt, B., et al. (2011). EPOXI: Comet 103P/Hartley 2 observations from a worldwide campaign. Astrophys. J. *734*, L1. https://doi.org/10.1088/2041-8205/734/1/L1.

222. Campins, H., Licandro, J., Pinilla-Alonso, N., Ziffer, J., León, J.d., Mothé-Diniz, T., Guerra, J.C., and Hergenrother, C. (2007). Nuclear Spectra of Comet 28P Neujmin 1. Astron. J. *134*, 1626–1633. https://doi.org/10.1086/519974.

223. Busemann, H., Nguyen, A.N., Cody, G.D., Hoppe, P., Kilcoyne, A.D., Stroud, R.M., Zega, T.J., and Nittler, L.R. (2009). Ultra-primitive interplanetary dust particles from the comet 26P/Grigg–Skjellerup dust stream collection. Earth Planet. Sci. Lett. *288*, 44–57. https://doi.org/10.1016/J.EPSL.2009.09.007.

224. Ootsubo, T., Kawakita, H., and Shinnaka, Y. (2021). Mid-infrared observations of the nucleus of Comet P/2016 BA14 (PANSTARRS). Icarus *363*, 114425. https://doi.org/10.1016/J.ICARUS.2021.114425.

225. Kokhirova, G.I., Rakhmatullaeva, F.J., and Borisenko, S.A. (2021). Results of Photometric Observations of Comet P/2019 LD2 at the Sanglokh Observatory. Sol. Syst. Res. *55*, 402–408. https://doi.org/10.1134/S0038094621050038.

226. Davoisne, C., Djouadi, Z., Leroux, H., D'Hendecourt, L., Jones, A., and Deboffle, D. (2006). The origin of GEMS in IDPs as deduced from microstructural evolution of amorphous silicates with annealing. Astron. Astrophys. *448*, L1. https://doi.org/10.1051/0004-6361:200600002.

227. Nuth, J.A., Rietmeijer, F.J.M., and Hill, H.G.M. (2002). Condensation processes in astrophysical environments: The composition and structure of cometary grains. Meteorit. Planet. Sci. *37*, 1579–1590. https://doi.org/10.1111/J.1945-5100.2002.TB00812.X.

228. Nuth, J.A., and Johnson, N.M. (2006). Crystalline silicates in comets: how did they form? Icarus *180*, 243–250. https://doi.org/10.1016/j.icarus.2005.09.003.

229. Messenger, S., Keller, L.P., Stadermann, F.J., Walker, R.M., and Zinner, E. (2003). Samples of stars beyond the solar system: Silicate grains in interplanetary dust. Science *300*, 105–108. https://doi.org/10.1126/SCIENCE.1080576.

230. Ciesla, F.J. (2007). Outward transport of high-temperature materials around the midplane of the solar nebula. Science *318*, 613–615. https://doi.org/10.1126/SCIENCE.1147273.

231. Bockelée–Morvan, D., Gautier, D., Hersant, F., Huré, J.M., and Robert, F. (2002). Turbulent radial mixing in the solar nebula as the source of crystalline silicates in comets. Astron. Astrophys. *384*, 1107–1118. https://doi.org/10.1051/0004-6361:20020086.

232. Cuzzi, J.N., Davis, S.S., and Dobrovolskis, A.R. (2003). Blowing in the wind. II. Creation and redistribution of refractory inclusions in a turbulent protoplanetary nebula. Icarus *166*, 385–402. https://doi.org/10.1016/J.ICARUS.2003.08.016.

233. Fukuda, K., Brownlee, D.E., Joswiak, D.J., Tenner, T.J., Kimura, M., and Kita, N.T. (2021). Correlated isotopic and chemical evidence for condensation origins of olivine in comet 81P/Wild 2 and in AOAs from CV and CO chondrites. Geochim. Cosmochim. Acta *293*, 544–574. https://doi.org/10.1016/J.GCA.2020.09.036.

234. Bouwman, J., de Koter, A., Dominik, C., and Waters, L.B.F.M. (2003). The origin of crystalline silicates in the Herbig Be star HD 100546 and in comet Hale-Bopp. Astron. Astrophys. *401*, 577–592. https://doi.org/10.1051/0004-6361:20030043.

235. Mulders, G.D., Waters, L.B.F.M., Dominik, C., Sturm, B., Bouwman, J., Min, M., Verhoeff, A.P., Acke, B., Augereau, J.C., Evans, N.J., et al. (2011). Low abundance, strong features: window-dressing crystalline forsterite in the disk wall of HD 100546. Astron. Astrophys. *531*, A93. https://doi.org/10.1051/0004-6361/201116770.

236. Brucato, J.R., Strazzulla, G., Baratta, G., and Colangeli, L. (2004). Forsterite amorphisation by ion irradiation: Monitoring by infrared spectroscopy. Astron. Astrophys. *413*, 395–401. https://doi.org/10.1051/0004-6361:20031574.

237. Demyk, K., Carrez, P., Leroux, H., Cordier, P., Jones, A.P., Borg, J., Quirico, E., Raynal, P.I., and D'Hendecourt, L. (2001). Structural and chemical alteration of crystalline olivine under low energy He+ irradiation. Astron. Astrophys. *368*, L38–L41. https://doi.org/10.1051/0004-6361:20010208.

238. Demyk, K., D'Hendecourt, L., Leroux, H., Jones, A.P., and Borg, J. (2004). IR spectroscopic study of olivine, enstatite and diopside irradiated with low energy H+ and He+ ions. Astron. Astrophys. *420*, 233–243. https://doi.org/10.1051/0004-6361:20040091.

239. Bringa, E.M., Kucheyev, S.O., Loeffler, M.J., Baragiola, R.A., Tielens, A.G.G.M., Dai, Z.R., Graham, G., Bajt, S., Bradley, J.P., Dukes, C.A., et al. (2007). Energetic Processing of Interstellar Silicate Grains by Cosmic Rays. Astrophys. J. *662*, 372–378. https://doi.org/10.1086/517865.

240. Kemper, F., Vriend, W.J., and Tielens, A.G.G.M. (2004). The Absence of Crystalline Silicates in the Diffuse Interstellar Medium. Astrophys. J. *609*, 826–837. https://doi.org/10.1086/421339.

241. Wooden, D., Butner, H.M., Harker, D.E., and Woodward, C.E. (2000). Mg-Rich Silicate Crystals in Comet Hale–Bopp: ISM Relics or Solar Nebula Condensates? Icarus *143*, 126–137. https://doi.org/10.1006/ICAR.1999.6240.

242. Messenger, S., Keller, L.P., and Lauretta, D.S. (2005). Geochemistry: Supernova olivine from cometary dust. Science *309*, 737–741. https://doi.org/10.1126/SCIENCE.1109602.

243. Higuchi, A., and Kokubo, E. (2019). Hyperbolic orbits in the Solar system: interstellar origin or perturbed Oort cloud comets? Mon. Not. R. Astron. Soc. *492*, 268–275. https://doi.org/10.1093/MNRAS/STZ3153.

244. Emel'yanenko, V.V., and Bailey, M.E. (1998). Capture of Halley-type comets from the near-parabolic flux. Mon. Not. R. Astron. Soc. *298*, 212–222. https://doi.org/10.1046/J.1365-8711.1998.01628.X.

245. Lyttleton, R.A. (1968). On the Distribution of Major-Axes of Long-Period Comets. Mon. Not. R. Astron. Soc. *139*, 225–230. https://doi.org/10.1093/MNRAS/139.2.225.

246. Oort, J.H. (1950). The structure of the cloud of comets surrounding the solar system and a hypothesis concerning its origin. Bull. Astron. Inst. Nethertands *11*, 91–110.

247. Nabiyev, S., Yalim, J., Guliyev, A., and Guliyev, R. (2022). Hyperbolic comets as an indicator of a hypothetical planet 9 in the solar system. Adv. Space Res. *69*, 3182–3203. https://doi.org/10.1016/J.ASR.2022.02.001.

248. Batygin, K., and Brown, M.E. (2016). Evidence for a distant giant planet in the solar system. Astron. J. *151*, 22. https://doi.org/10.3847/0004-6256/151/2/22.

249. Bromley, B.C., and Kenyon, S.J. (2016). Making planet nine: a scattered giant in the outer solar system. Astrophys. J. *826*, 64. https://doi.org/10.3847/0004-637X/826/1/64.

250. Trujillo, C.A., and Sheppard, S.S. (2014). A Sedna-like body with a perihelion of 80 astronomical units. Nature *507*, 471–474. https://doi.org/10.1038/nature13156.

251. Kimura, Y., and Nuth, J.A. (2009). A seed of solar forsterite and possible new evolutional scenario of cosmic silicates. Astrophys. J. *697*, L10–L13. https://doi.org/10.1088/0004-637X/697/1/L10.

252. Meibom, A., Desch, S.J., Krot, A.N., Cuzzi, J.N., Petaev, M.I., Wilson, L., and Keil, K. (2000). Large-scale thermal events in the solar nebula: Evidence from Fe,Ni metal grains in primitive meteorites. Science *288*, 839–841. https://doi.org/10.1126/SCIENCE.288.5467.839.

253. Podosek, F.A., and Cassen, P. (1994). Theoretical, observational, and isotopic estimates of the lifetime of the solar nebula. Meteoritics *29*, 6–25. https://doi.org/10.1111/J.1945-5100.1994.TB00649.X.

254. Stolper, E., and Paque, J.M. (1986). Crystallization sequences of Ca-Al-rich inclusions from Allende: The effects of cooling rate and maximum temperature. Geochim. Cosmochim. Acta *50*, 1785–1806. https://doi.org/10.1016/0016-7037(86)90139-0.

255. de Koker, N.P., Stixrude, L., and Karki, B.B. (2008). Thermodynamics, structure, dynamics, and freezing of Mg2SiO4 liquid at high pressure. Geochim. Cosmochim. Acta *72*, 1427–1441. https://doi.org/10.1016/J.GCA.2007.12.019.

256. Han, J., and Brearley, A.J. (2015). Microstructural evidence for complex formation histories of amoeboid olivine aggregates from the ALHA77307 CO3.0 chondrite. Meteorit. Planet. Sci. *50*, 904–925. https://doi.org/10.1111/MAPS.12439.

257. Marrocchi, Y., Villeneuve, J., Jacquet, E., Piralla, M., and Chaussidon, M. (2019). Rapid condensation of the first Solar System solids. Proc. Natl. Acad. Sci. USA *116*, 23461–23466. https://doi.org/10.1073/PNAS.1912479116.

258. Krot, A.N. (2019). Refractory inclusions in carbonaceous chondrites: Records of early solar system processes. Meteorit. Planet. Sci. *54*, 1647–1691. https://doi.org/10.1111/MAPS.13350.

259. Sugiura, N., Petaev, M.I., Kimura, M., Miyazaki, A., and Hiyagon, H. (2009). Nebular history of amoeboid olivine aggregates. Meteorit. Planet. Sci. *44*, 559–572. https://doi.org/10.1111/J.1945-5100.2009.TB00751.X.

260. Ruzicka, A., Floss, C., and Hutson, M. (2012). Amoeboid olivine aggregates (AOAs) in the Efremovka, Leoville and Vigarano (CV3) chondrites: A record of condensate evolution in the solar nebula. Geochim. Cosmochim. Acta *79*, 79–105. https://doi.org/10.1016/J.GCA.2011.11.043.

261. Nguyen, A.N., and Zinner, E. (2004). Discovery of Ancient Silicate Stardust in a Meteorite. Science *303*, 1496–1499. https://doi.org/10.1126/SCIENCE.1094389.

262. Trinquier, A., Elliott, T., Ulfbeck, D., Coath, C., Krot, A.N., and Bizzarro, M. (2009). Origin of nucleosynthetic isotope heterogeneity in the solar protoplanetary disk. Science *324*, 374–376. https://doi.org/10.1126/SCIENCE.1168221.

263. Singerling, S.A., Nittler, L.R., Barosch, J., Dobrică, E., Brearley, A.J., and Stroud, R.M. (2023). Tracing the history of an unusual compound presolar grain from progenitor star to asteroid parent body host. Geochim. Cosmochim. Acta *344*, 230–243. https://doi.org/10.1016/J.GCA.2023.01.015.

264. Hu, J.Y., Dauphas, N., Tissot, F.L.H., Yokochi, R., Ireland, T.J., Zhang, Z., Davis, A.M., Ciesla, F.J., Grossman, L., Charlier, B.L.A., et al. (2021). Heating events in the nascent solar system recorded by rare earth element isotopic fractionation in refractory inclusions. Sci. Adv. *7*. https://doi.org/10.1126/SCIADV.ABC2962.

265. Herbig, G.H. (1977). Eruptive phenomena in early stellar evolution. ApJ *217*, 693–715. https://doi.org/10.1086/155615.

266. Salmeron, R., and Ireland, T. (2012). The role of protostellar jets in star formation and the evolution of the early solar system: Astrophysical and meteoritical perspectives. Meteorit. Planet. Sci. *47*, 1922–1940. https://doi.org/10.1111/MAPS.12029.

267. Krot, A.N., Yurimoto, H., Hutcheon, I.D., and MacPherson, G.J. (2005). Chronology of the early Solar System from chondrule-bearing calcium-aluminium-rich inclusions. Nature *434*, 998–1001. https://doi.org/10.1038/nature03470.

268. Krot, A.N., Park, C., and Nagashima, K. (2014). Amoeboid olivine aggregates from CH carbonaceous chondrites. Geochim. Cosmochim. Acta *139*, 131–153. https://doi.org/10.1016/J.GCA.2014.04.050.

269. Sugiura, N., and Krot, A.N. (2007). 26Al-26Mg systematics of Ca-Al-rich inclusions, amoeboid olivine aggregates, and chondrules from the ungrouped carbonaceous chondrite Acfer 094. Meteorit. Planet. Sci. *42*, 1183–1195. https://doi.org/10.1111/J.1945-5100.2007.TB00568.X.

270. Connelly, J.N., Bizzarro, M., Krot, A.N., Nordlund, Å., Wielandt, D., and Ivanova, M.A. (2012). The absolute chronology and thermal processing of solids in the solar protoplanetary disk. Science *338*, 651–655. https://doi.org/10.1126/SCIENCE.1226919.

271. Alibert, Y., Mousis, O., Mordasini, C., and Benz, W. (2005). New Jupiter and Saturn Formation Models Meet Observations. Astrophys. J. *626*, L57–L60. https://doi.org/10.1086/431325.

272. Wood, B.J., Walter, M.J., and Wade, J. (2006). Accretion of the Earth and segregation of its core. Nature *441*, 825–833. https://doi.org/10.1038/nature04763.

273. Nakagawa, Y., Hayashi, C., and Nakazawa, K. (1983). Accumulation of planetesimals in the solar nebula. Icarus *54*, 361–376. https://doi.org/10.1016/0019-1035(83)90234-8.

274. Marrocchi, Y., Euverte, R., Villeneuve, J., Batanova, V., Welsch, B., Ferrière, L., and Jacquet, E. (2019). Formation of CV chondrules by recycling of amoeboid olivine aggregate-like precursors. Geochim. Cosmochim. Acta *247*, 121–141. https://doi.org/10.1016/J.GCA.2018.12.038.

275. Han, J., Park, C., and Brearley, A.J. (2022). A record of low-temperature asteroidal processes of amoeboid olivine aggregates from the Kainsaz CO3.2 chondrite. Geochim. Cosmochim. Acta *322*, 109–128. https://doi.org/10.1016/J.GCA.2022.02.007.

276. Dauphas, N., and Chaussidon, M. (2011). A Perspective from Extinct Radionuclides on a Young Stellar Object: The Sun and Its Accretion Disk. Annu. Rev. Earth Planet. Sci. *39*, 351–386. https://doi.org/10.1146/ANNUREV-EARTH-040610-133428.

277. Ysard, N., Köhler, M., Jones, A., Miville-Deschênes, M.A., Abergel, A., and Fanciullo, L. (2015). Dust variations in the diffuse interstellar medium: constraints on Milky Way dust from Planck-HFI observations. Astron. Astrophys. *577*, A110. https://doi.org/10.1051/0004-6361/201425523.

278. Leone, G., Bieger, K., and Soto, M. (2021). Identification of Possible Heat Sources for the Thermal Output of Enceladus. Planet. Sci. J. *2*, 29. https://doi.org/10.3847/PSJ/abdb33.

279. Umebayashi, T., and Nakano, T. (2008). Effects of radionuclides on the ionization state of protoplanetary disks and dense cloud cores. Astrophys. J. *690*, 69–81. https://doi.org/10.1088/0004-637X/690/1/69.

280. Leone, G., Tanaka, H.K.M., Holma, M., Kuusiniemi, P., Varga, D., Oláh, L., Presti, D.L., Ferlito, C., Gallo, G., Monaco, C., et al. (2021). Muography as a new complementary tool in monitoring volcanic hazard: implications for early warning systems. Proc. R. Soc. A *477*, 20210320. https://doi.org/10.1098/RSPA.2021.0320.

281. Morishima, K., Kuno, M., Nishio, A., Kitagawa, N., Manabe, Y., Moto, M., Takasaki, F., Fujii, H., Satoh, K., Kodama, H., et al. (2017). Discovery of a big void in Khufu's Pyramid by observation of cosmic-ray muons. Nature *552*, 386–390. https://doi.org/10.1038/nature24647.

282. Tanaka, H.K.M., Aichi, M., Balogh, S.J., Bozza, C., Coniglione, R., Gluyas, J., Hayashi, N., Holma, M., Joutsenvaara, J., Kamoshida, O., et al. (2022). Periodic sea-level oscillation in Tokyo Bay detected with the Tokyo-Bay seafloor hyper-kilometric submarine deep detector (TS-HKMSDD). Sci. Rep. *12*, 6097. https://doi.org/10.1038/s41598-022-10078-2.

283. Prettyman, T. (2019). Deep Mapping of Small Solar System Bodies with Galactic Cosmic Ray Secondary Particle Showers (NASA Technical Reports Server (NTRS)).

284. Gaisser, T.K., Engel, R., and Resconi, E. (2016). Cosmic Rays and Particle Physics Cambridge Universit (Cambridge University Press).

285. Preibisch, T., and Feigelson, E.D. (2005). The Evolution of X-Ray Emission in Young Stars. Astrophys. J. Suppl. Ser. *160*, 390–400. https://doi.org/10.1086/432094.

286. Wuchterl, G., and Klessen, R.S. (2001). The First Million Years of the Sun: A Calculation of the Formation and Early Evolution of a Solar Mass Star. Astrophys. J. *560*, L185–L188. https://doi.org/10.1086/324307.

287. Kaminski, E., Limare, A., Kenda, B., and Chaussidon, M. (2020). Early accretion of planetesimals unraveled by the thermal evolution of the parent bodies of magmatic iron meteorites. Earth Planet. Sci. Lett. *548*, 116469. https://doi.org/10.1016/J.EPSL.2020.116469.

288. Chambers, J.E. (2004). Planetary accretion in the inner Solar System. Earth Planet. Sci. Lett. *223*, 241–252. https://doi.org/10.1016/J.EPSL.2004.04.031.

289. Pape, J., Mezger, K., Bouvier, A.S., and Baumgartner, L.P. (2019). Time and duration of chondrule formation: Constraints from 26Al-26Mg ages of individual chondrules. Geochim. Cosmochim. Acta *244*, 416–436. https://doi.org/10.1016/J.GCA.2018.10.017.

290. Sasaki, S., and Nakazawa, K. (1990). Did a primary solar-type atmosphere exist around the proto-earth? Icarus *85*, 21–42. https://doi.org/10.1016/0019-1035(90)90101-E.

291. Canup, R.M. (2008). Accretion of the Earth. Philos. Trans. A Math. Phys. Eng. Sci. *366*, 4061–4075. https://doi.org/10.1098/RSTA.2008.0101.

292. Malamud, U., Perets, H.B., and Schubert, G. (2017). The contraction/expansion history of Charon with implications for its planetary-scale tectonic belt. Mon. Not. R. Astron. Soc. *468*, 1056–1069. https://doi.org/10.1093/MNRAS/STX546.

293. Kenyon, S.J., and Bromley, B.C. (2012). Coagulation calculations of icy planet formation at 15–150 au: a correlation between the maximum radius and the slope of the size distribution for trans-neptunian objects. Astron. J. *143*, 63. https://doi.org/10.1088/0004-6256/143/3/63.